



HAL
open science

Interchromosomal contacts between regulatory regions trigger stable transgenerational epigenetic inheritance in *Drosophila*

Maximilian Fitz-James, Gonzalo Sabarís, Peter Sarkies, Frédéric Bantignies,
Giacomo Cavalli

► To cite this version:

Maximilian Fitz-James, Gonzalo Sabarís, Peter Sarkies, Frédéric Bantignies, Giacomo Cavalli. Interchromosomal contacts between regulatory regions trigger stable transgenerational epigenetic inheritance in *Drosophila*. 2023. hal-04252150

HAL Id: hal-04252150

<https://hal.umontpellier.fr/hal-04252150>

Preprint submitted on 20 Oct 2023

HAL is a multi-disciplinary open access archive for the deposit and dissemination of scientific research documents, whether they are published or not. The documents may come from teaching and research institutions in France or abroad, or from public or private research centers.

L'archive ouverte pluridisciplinaire **HAL**, est destinée au dépôt et à la diffusion de documents scientifiques de niveau recherche, publiés ou non, émanant des établissements d'enseignement et de recherche français ou étrangers, des laboratoires publics ou privés.

1 Interchromosomal contacts between regulatory regions trigger stable 2 transgenerational epigenetic inheritance in *Drosophila*

3 Maximilian H. Fitz-James¹, Gonzalo Sabarís¹, Peter Sarkies², Frédéric Bantignies¹, Giacomo
4 Cavalli^{1*}

5 ¹Institute of Human Genetics, CNRS and University of Montpellier, 141 Rue de la Cardonille,
6 34094 Montpellier, France

7 ²Department of Biochemistry, University of Oxford, South Parks Road, Oxford OX1 3QU, UK

8 *Corresponding Author: e-mail: giacomo.cavalli@igh.cnrs.fr ; Phone: +33-4344359970; Fax
9 +33-434359901

10

11 Summary

12 Non-genetic information can be inherited across generations by the process of
13 Transgenerational Epigenetic Inheritance (TEI). TEI can be established by various triggering
14 events, including transient genetic perturbations. In *Drosophila*, hemizyosity of the *Fab-7*
15 regulatory element triggers inheritance of the histone mark H3K27me3 at a homologous locus
16 on another chromosome, resulting in heritable epigenetic differences in eye colour. By mutating
17 transcription factor binding sites within the *Fab-7* element, we demonstrate the importance of
18 two proteins in the establishment and maintenance of TEI: GAGA-factor and Pleiohomeotic. We
19 show that these proteins function by recruiting the Polycomb Repressive Complex 2 and by
20 mediating interchromosomal chromatin contacts between *Fab-7* and its homologous locus.
21 Finally, using an *in vivo* synthetic biology system to induce them, we show that chromatin
22 contacts alone can establish TEI, providing a mechanism by which hemizyosity of one locus
23 can establish epigenetic memory at another *in trans* through long-distance chromatin contacts.

24

25 Keywords

26 Transgenerational Epigenetic Inheritance ; Chromatin Contacts ; Genome Organisation ;
27 Epimutation ; Polycomb ; GAGA-Factor ; *Fab-7*

28

29 Introduction

30 Epigenetic information has long been known to be a major factor in the regulation of gene
31 expression¹. Whether such information can be transmitted across generations in various
32 organisms has been a more elusive question, made difficult by the potential for genetic factors
33 to confound experiments on heredity^{2,3}. Through careful experimentation in model organisms,
34 recent work has now demonstrated that such transgenerational epigenetic inheritance (TEI)
35 does occur in a variety of organisms^{4,5}. In addition, although much more work is required, the
36 molecular mechanisms underlying these instances of inheritance have begun to be described⁶.
37 Many of the most well-known epigenetic regulators of gene expression have been implicated in
38 different cases of TEI, including non-coding RNAs⁷⁻¹², DNA methylation¹³⁻¹⁵ and histone
39 modifications^{12,16-19}, while less typical sources of non-genetic information, such as 3D chromatin
40 organisation¹⁹ and transcription factor binding²⁰, have been suggested as secondary signals in
41 some cases.

42 Just as genes and their allelic variants are the basis of genetic variation, so are “epialleles” the
43 basic units of heritable epigenetic change. Similarly, while mutation is the means by which
44 genetic variation arises, “epimutation” describes the appearance of a heritable change in
45 epigenetic information that gives rise to an epiallele. Epimutation provides an alternative source
46 of heritable variation which differs from genetic mutation in that it has the potential to be more
47 rapid, targeted and reversible, allowing for fast adaptation to a fluctuating environment²¹.
48 Nonetheless, the underlying causes of epimutation and the mechanism by which they arise
49 remain unclear and likely vary between organisms.

50 Given the complexity of mechanisms involved in TEI in higher eukaryotes, model systems that
51 can be easily manipulated and allow one to both effectively track heritable phenotypes and
52 analyse the underlying molecular events at play are critically needed in the field. One clear
53 example of TEI occurs in *Drosophila melanogaster*, in a transgenic line called “Fab2L”, involving
54 a transgene that drives the expression of the eye pigmentation gene *mini-white*²². Flies of the
55 Fab2L line exhibit a stochastic phenotype, manifesting as mosaicism of pigmentation in the
56 adult eye. A memory of this phenotype can be established by a transient genetic perturbation¹⁹
57 which can then be maintained epigenetically for countless generations following the initial
58 trigger. While this represents a clear case of TEI, its molecular mechanisms remain mysterious,
59 making it a valuable model system to study the means by which heritable epigenetic variability
60 arises. Here, we investigate the mechanistic basis for the establishment of transgenerational
61 epigenetic inheritance at the Fab2L locus. We show that it is mediated by two key regulatory

62 regions of the transgene through the binding of the transcription factors GAGA-factor (GAF) and
63 Pleiohomeotic (Pho). We show that these transcription factors recruit the Polycomb Repressive
64 Complex 2 (PRC2) to the transgene, leading to deposition of H3K27me3, and promote
65 interchromosomal chromatin contacts between the transgene and a homologous region
66 elsewhere in the genome. Using an *in vivo* synthetic biology system, we artificially recapitulate
67 these contacts to demonstrate that chromatin contacts alone are sufficient to induce TEI in
68 *Drosophila*, providing a mechanism whereby genetic perturbation of one locus can trigger TEI at
69 another *in trans* through long-distance chromatin interactions.

70

71 **Results**

72 **Binding of GAGA-Factor and Pho is responsible for epigenetic variability at the Fab2L** 73 **transgene**

74 The *Drosophila* Fab2L line carries a single copy 12.4kb transgene inserted into chromosome
75 arm 2L at cytogenetic position 37B^{22,23}. This transgene contains the reporter genes *LacZ* and
76 *mini-white* under the control of the *Fab-7* element. *Fab-7* is a well-studied regulatory region of
77 the bithorax complex on chromosome 3, where it regulates the expression of the Hox gene *Abd-*
78 *b*²⁴⁻²⁶. Importantly, the Fab2L line therefore contains two versions of the *Fab-7* element in its
79 genome, one at its endogenous location on chromosome 3 and one inserted ectopically within
80 the transgene on chromosome 2 (Figure 1A).

81 The *mini-white* reporter gene, which controls red pigment deposition in the eye, is not expressed
82 uniformly in Fab2L flies but shows a mosaic pattern of eye pigmentation, with some ommatidia
83 showing strong *mini-white* expression and others strong repression, within the same individual
84 (Figure S1A,B). Stochastic binding of the Polycomb Repressive Complex 2 (PRC2), resulting in
85 deposition of the repressive histone mark H3K27me3, has been suggested as an explanation
86 for the variability of mini-white expression in transgenes carrying Polycomb-bound elements.
87 This mosaic eye pattern therefore represents a very evident and visible instance of epigenetic
88 variation in the absence of any underlying genetic change¹⁹.

89 To further investigate the mechanism behind this epigenetic variation, we generated transgenic
90 versions of the Fab2L transgene with mutations in key sequence motifs in the *Fab-7* element.
91 *Fab-7* contains within it two important subdomains: an insulator region, which in its endogenous
92 state prevents mis-regulation of *Abd-B* by adjacent regulatory regions in the wrong body

93 segments, and a Polycomb Response Element (PRE), which recruits either Polycomb Group
94 (PcG) or Trithorax Group (TrxG) proteins to maintain the pattern of *Abd-B* expression
95 established early in development. Both of these regions contain several consensus sequence
96 motifs for the DNA-binding proteins GAF and Pho (Figure 1B). Among other functions, both of
97 these proteins are known to be recruiters of PRC2, strongly suggesting their potential
98 involvement in the variable H3K27me3 levels, and thus the eye colour phenotype, in Fab2L.

99 We generated three transgenic lines mutating all GAF and Pho sequence motifs within either
100 the insulator (Fab2L-INS), the PRE (Fab2L-PRE) or both (Fab2L-INS-PRE) in the Fab2L
101 transgene (Figure 1B). Fab2L-INS showed a significant decrease in GAF binding to the
102 insulator, although Pho binding was little affected as was GAF binding to the PRE. Interestingly,
103 Fab2L-PRE had the opposite effect, with GAF binding at both sites unaffected, while Pho
104 binding was significantly decreased at the PRE only (Figure 1C,D). These results extended to
105 the recruitment of PRC2 to Fab2L, which was largely unaffected in Fab2L-INS but significantly
106 decreased in Fab2L-PRE, not only at the PRE itself but also exterior to the *Fab-7* at the
107 downstream LacZ region (Figure 1E). Mutation of both regions together shows clear additive
108 effects. Indeed, in the Fab2L-INS-PRE line binding of both GAF and Pho are decreased at both
109 the insulator and PRE, and in most cases to a significantly greater extent than in either of the
110 single mutants (Figure 1C,D), although PRC2 binding was not significantly different from Fab2L-
111 PRE (Figure 1E). Taken together, these results suggest that the insulator and PRE regions of
112 *Fab-7* act cooperatively to recruit GAF and Pho to the Fab2L transgene, although the PRE may
113 play the greater role in the subsequent recruitment of PRC2.

114 We then analysed the downstream effects of this altered GAF and Pho recruitment on the
115 chromatin and phenotype of the mutant lines. All three mutant lines had significantly decreased
116 levels of H3K27me3 across the transgene, with the decrease being much more pronounced in
117 the double mutant Fab2L-INS-PRE line (Figure 1F). These changes in chromatin translated to
118 phenotypic effects on the eye colour of the adult flies. Indeed, all three mutant lines displayed
119 shifts towards red eye colour compared to naïve Fab2L (Figures 1G-J and S1). While it
120 remained considerable, the shift in Fab2L-INS was milder than for the other two lines, with
121 approximately 16% of females and 61% of males exhibiting fully red eyes (Figures 1H and
122 S1C,D). In contrast, almost all Fab2L-PRE and Fab2L-INS-PRE flies of both sexes exhibited
123 fully red eyes. It is interesting to note, however, that while the shift towards red was complete for
124 Fab2L-INS-PRE, with all individuals having uniform red eyes (Figures 1J and S1G,H), Fab2L-
125 PRE retained some stochasticity, with around 7% of females possessing at least some white

126 ommatidia (Figures 1I and S1E). These results reinforce the idea that the insulator and PRE
127 together are responsible for the epigenetic and phenotypic variability of the Fab2L fly line.

128

129 **The insulator and PRE regions of *Fab-7* are individually sufficient to mediate epigenetic** 130 **inheritance**

131 In WT flies carrying the Fab2L transgene, epigenetic differences in expression between
132 individuals are not inherited transgenerationally under normal conditions. . Indeed, when we
133 applied repeated selection and crossing of the most extreme individuals in the population of an
134 unmanipulated Fab2L line over ten generations, we did not obtain any significant differences in
135 eye colour across the population (Figure S2A,B). However, crossing this “naïve” Fab2L line with
136 another Fab2L line bearing a homozygous deletion of the endogenous *Fab-7* gives F1
137 individuals carrying the transgene in a homozygous state, but the endogenous *Fab-7* in a
138 hemizygous state (Figure S2C). This hemizyosity establishes transgenerational epigenetic
139 memory at the transgene, such that reconstituting the Fab2L genotype in the F2 results in a line
140 which is genetically identical to the P0 Fab2L, but in which TEI is now possible¹⁹. Indeed,
141 selection of this line over 10 generations resulted in either red or white “epilines”: populations of
142 flies with a significant proportion of individuals with monochrome eye colour, i.e. with 100% of
143 their ommatidia either pigmented or unpigmented (Figure S2D). We also found that other
144 crossing schemes which induced *Fab-7* hemizyosity for one or two generations, were able to
145 trigger TEI in Fab2L (Figure S2E-J).

146 Given the altered phenotype of the mutant Fab2L transgenic lines, we asked whether these
147 mutations also interfered with the ability of the Fab2L transgene to maintain a memory of its
148 epigenetic state across generations by TEI. Due to the shift towards red eyes in the naïve
149 Fab2L-INS, Fab2L-PRE and Fab2L-INS-PRE lines, selection towards red eyes would not be
150 informative. We therefore performed a transgenerational epigenetic selection experiment to
151 determine if these mutant lines could be selected towards a more repressed, white-eyed
152 phenotype than the naïve population. Just as with wild-type Fab2L (Figure S2C), we introduced
153 a single generation of *Fab-7* hemizyosity while leaving the mutant versions of the Fab2L
154 transgene unmanipulated (Figure 2A). We then reconstituted the parental genotype,
155 homozygous for the endogenous *Fab-7*, and selectively bred the most white-eyed individuals
156 over subsequent generations. As a control, we used a wild-type Fab2L line which had
157 previously been selected for a red-eyed phenotype. The Fab2L, Fab2L-INS and Fab2L-PRE,

158 which all showed a greater or lesser degree of variability in their starting populations, were
159 receptive to selection, showing a clear and gradual shift towards whiter eyes in both females
160 and males over the generations (Figures 2B-D and S3A-C). In the case of Fab2L-INS, the
161 appearance of some individuals with fully white eyes was even observed (Figures 2C and S3B),
162 consistent with the less extreme de-repression observed in this line compared to the other
163 mutants. In contrast, the Fab2L-INS-PRE line displayed no variation at any point during the
164 experiment, with all individuals of both sexes maintaining a uniform red eye colour (Figures 2D
165 and S3C). As expected, some pre-existing degree of Polycomb binding and some form of
166 epigenetic variation at the Fab2L transgene is therefore prerequisite for TEI. However, these
167 results also demonstrate that the insulator or PRE regions alone are still able to mediate TEI,
168 indicating that they act together to maintain an epigenetic memory at the transgenic *Fab-7*
169 element in the Fab2L line.

170

171 **The insulator and PRE regions of *Fab-7* are required for horizontal transmission of a**
172 **repressed epigenetic state through paramutation**

173 The Fab2L transgene is not only able to acquire an altered epigenetic state by selection over
174 generations, but can do so in a single generation by the process of “paramutation”¹⁹.
175 Paramutation denotes the horizontal transfer of an epigenetic state *in trans* between two
176 homologous alleles, and has been described in many organisms including *Drosophila*^{27–30}. In
177 the Fab2L line, crossing a naïve Fab2L with an established Fab2L epilene (either white or red-
178 eyed) results in the acquisition by the naïve allele of the altered epigenetic state of the epilene
179 allele. This phenomenon can be tracked by the use of a *black[1]* marker allele, closely linked to
180 the Fab2L transgene, such that F2 individuals that have inherited both copies of Fab2L from the
181 naïve parent can be determined with high probability (Figures 3A and S4A). Although these F2
182 flies possess the genetic material of the naïve P0 population, their epigenetic state resembles
183 that of the epilene with which it was crossed, attesting to the acquisition over this genomic region
184 of a new epigenetic state (Figures 3B and S4B).

185 To determine if mutation of the transgene interfered with horizontal transfer of epigenetic state,
186 we crossed the Fab2L-INS, Fab2L-PRE and Fab2L-INS-PRE lines with a white-eyed Fab2L
187 epilene in order to see if these mutant versions of the Fab2L transgene could acquire a
188 repressed epigenetic state by paramutation in addition to, or instead of, selection over
189 generations. Again, as control we used a wild-type Fab2L epilene which had previously acquired

190 a de-repressed, red-eyed epigenetic state. Just as with the selection, Fab2L, Fab2L-INS and
191 Fab2L-PRE were able to acquire a more white-eyed phenotype than the naïve parental lines
192 (Figure 3C-E). Conversely, all Fab2L-INS-PRE individuals maintained their uniform red
193 coloration of the eyes even after exposure in the F1 of the cross to a repressed epiallele (Figure
194 3F). While lines bearing a wild-type version of the insulator or PRE of *Fab-7* alone were
195 therefore able to acquire an altered epigenetic state by both selection over generations and
196 paramutation, mutation of both regions together completely prevents acquisition of a repressed
197 epigenetic state by either method. Taken together, these results therefore suggest that the
198 insulator and PRE work together not only to mediate epigenetic variation at the transgenic *Fab-*
199 *7*, but also to maintain an epigenetic memory across generations.

200

201 **GAF mediates long-range chromatin contacts through the insulator region of *Fab-7***

202 Our results point to PRC2 and GAF as key factors mediating the epigenetic variability, and its
203 inheritance across generations, at the Fab2L transgene. PRC2 has a direct role in regulating the
204 expression of the Fab2L transgene, as the differences in *mini-white* expression and phenotype
205 of the Fab2L epilines correlate with differences in PRC2-deposited H3K27me3 across the
206 transgene¹⁹. The role of GAF is less clear as mutation of the GAF sites in the insulator ultimately
207 had little effect on PRC2 binding (Figure 1E), suggesting that GAF's primary role at the *Fab-7*
208 element may not be the recruitment of PRC2. Intriguingly, among its many other functions, GAF
209 has been shown to mediate long-range chromatin contacts between its target genes³¹⁻³³. The
210 three-dimensional organization of chromatin is a major factor in the regulation of gene
211 expression, and polycomb target genes in particular are frequently found to colocalize in the
212 nucleus at so-called "Polycomb bodies"³⁴. Moreover, the transgenic and endogenous copies of
213 *Fab-7* were previously found to form chromatin contacts in the Fab2L line¹⁹.

214 To quantify these chromatin contacts, we performed Fluorescence in situ hybridisation (FISH) to
215 visualise the regions surrounding the *Fab-7* elements in Fab2L embryos carrying different copy
216 numbers of the endogenous *Fab-7* (Figure 4A,B). These regions showed significant
217 colocalization in the nuclei of Fab2L embryos, but not in Fab2L ; *Fab7[1]* embryos which lack
218 the endogenous *Fab-7*. This shows that chromatin contacts do occur between these loci
219 dependent on the presence of both *Fab-7* elements. Intriguingly, the Fab2L-*Fab-7* chromatin
220 contacts observed in Fab2L increase even further in a *Fab7[1]/+* genetic background in which
221 only one copy of the endogenous *Fab-7* is present.

222 To investigate the effect of Fab2L mutation on these chromatin contacts, we extended the FISH
223 analysis to our mutated transgenic lines (Figures 4C-G and S5). In both a homozygous and
224 hemizygous *Fab-7* background, chromatin contacts between Fab2L and *Fab-7* were
225 comparable between Fab2L-PRE and wild-type Fab2L. This is measured both in a similar
226 average distance between the two loci (Figure 4D,F) and in the proportion of nuclei in which the
227 loci are in close proximity (Figure 4E,G). Conversely, contacts are significantly decreased in
228 Fab2L-INS compared to wild-type Fab2L, suggesting a primary role for the insulator, and GAF,
229 in mediating these chromatin contacts. It is worth noting, however, that mutation of the insulator
230 does not fully abrogate chromatin contacts to the extent seen in Fab2L ; *Fab7[1]*, whereas
231 mutation of both the insulator and PRE does. Thus, while Fab2L-PRE is not significantly
232 different from Fab2L, and Fab2L-INS-PRE is not significantly different from Fab2L ; *Fab7[1]*,
233 Fab2L-INS displays an intermediate phenotype, indicating significant, but not complete, loss of
234 contacts between the two loci (Figure 4D-G, and S5C,G). Taken together, these results strongly
235 suggest that contacts between the *Fab-7* elements are primarily mediated through the insulator
236 region, but that the PRE may also play a stabilizing role.

237

238 **Artificially-induced chromatin contacts are sufficient to induce TEI at the Fab2L locus**

239 We then sought to investigate whether chromatin contacts may play a causal role in the
240 establishment of TEI at Fab2L. Inter-loci Fab2L-*Fab-7* distance does not differ significantly
241 between white- or red-eyed epilines of Fab2L¹⁹, arguing against a contribution of chromatin
242 contacts to the maintenance of epigenetic differences between these epilines. We also found
243 that while these contacts are robust in late-stage embryos (stage 14-15) they are not observable
244 in early stages (stage 4-5) (Figure S6), indicating that chromatin contacts themselves are
245 unlikely to be the transgenerationally inherited signal of TEI. However, the increase in Fab2L-
246 *Fab-7* chromatin contacts in Fab2L ; *Fab7[1]*/+ individuals hemizygous for the endogenous *Fab-*
247 *7* (Figure 4A), correlating with the triggering of TEI in the genetic crosses previously discussed
248 (Figure S2), makes the gain of chromatin contacts a prime candidate for the molecular trigger
249 that establishes TEI. We therefore wished to explore this correlation in greater detail.

250 To directly investigate the role of chromatin contacts in the triggering of TEI, we therefore
251 sought to induce contacts rather than abrogate them. To achieve this, we developed an *in vivo*
252 system to induce interchromosomal contacts between the two regions of interest without
253 recourse to any genetic perturbation. We dubbed this system “Three-Dimensional Contact

254 Induction System” or “3D-CIS”, for its ability to bring two distant loci in proximity (Figures 5A and
255 S7). To create this system, we inserted arrays of Lac or Tet operators adjacent to the transgenic
256 and endogenous *Fab-7* elements, respectively. Aside from the addition of these arrays, this line
257 has the same genotype as the Fab2L line, and has a similar average distance and contact
258 frequency between the two loci (Figures 5B,D,E and S8A). However, activation of the system by
259 introducing a TetR-LacI fusion protein which binds to both arrays (Figure S7E,F) results in
260 anchoring of the two *Fab-7* elements to each other (Figure 5C). This anchoring leads to a
261 decrease in the average Fab2L-*Fab-7* distance and increase in the frequency of close contacts,
262 both to levels comparable to the hemizygous Fab2L ; *Fab7[1]/+* in which TEI is established
263 (Figures 5D,E and S8B). Importantly, at no point are either the transgenic or endogenous *Fab-7*
264 in a hemizygous state (Figure S7A,B). The 3D-CIS system therefore allows us to investigate the
265 effect of increasing chromatin contacts between the two *Fab-7* elements in the absence of any
266 genetic perturbation.

267 Just as with Fab2L in the absence of genetic perturbation (Figure S2A,B), selection of the 3D-
268 CIS line in the “OFF” state over several generations did not result in any change in eye colour
269 across the population, towards either white or red eyes (Figure 5B,F). After ten generations of
270 selection, these lines also exhibited no difference in H3K27me3 levels between each other
271 (Figure 5I). However, activation of the 3D-CIS system, by introduction of the TetR-LacI fusion
272 protein and thus increase in contacts between the Fab2L transgene and endogenous *Fab-7*,
273 was able to establish TEI, such that selection over subsequent generations resulted in both
274 white and red epilines (Figure 5C,G). These epilines also had significant differences in
275 H3K27me3 levels between them (Figure 5J), reminiscent of the differences between Fab2L
276 epilines obtained by selection after transient hemizyosity of *Fab-7* (Figure 5H). These results
277 demonstrate that chromatin contacts alone, in the absence of any genetic perturbation, are
278 sufficient to induce TEI at the Fab2L transgene. As further controls, we generated two more
279 lines expressing either a LacI-LacI or a TetR-TetR fusion protein as part of the 3D-CIS system
280 (Figure S7C,D). These lines were also unable to trigger TEI (Figure S9), showing that triggering
281 is not due to expression of a fusion protein or its binding to either array singly, but conclusively
282 results from the binding of the fusion protein to both arrays in tandem.

283

284 **The *Fab-7* element is required for stable chromatin contacts**

285 The ability of the 3D-CIS system to induce TEI in Fab2L suggests that the primary role of the
286 *Fab-7* element in the establishment of TEI is to mediate long-range chromatin contacts between
287 the transgenic and endogenous *Fab-7* elements. To determine whether induced chromatin
288 contacts can trigger TEI at the Fab2L transgene even in the absence of the *Fab-7* element, we
289 generated a new version of the 3D-CIS system in which the transgenic *Fab-7* was deleted
290 (Figure S10A). As expected, phenotypically, this line resembled Fab2L-INS-PRE, with all
291 individuals possessing uniform red eyes (Figures 1J and S10B). Similarly, this LacO-Fab2L-
292 Fab7 Δ line was unable to acquire a repressed epigenetic state by either selection or
293 paramutation (Figure S10C-E). Activation of the 3D-CIS system by introduction of the LacI-TetR
294 fusion protein was also unable to trigger TEI in this line (Figure S10F-I). However, FISH analysis
295 revealed that chromatin contacts between the transgene and the endogenous *Fab-7* were not
296 increased in this line. Indeed in both the “OFF” and “ON” state, 3D-CIS-Fab7 Δ flies did not show
297 any significant contacts between the two loci, comparable to Fab2L ; *Fab7[1]* (Figure S10J).
298 This suggests that 3D-CIS is insufficient to mediate long-range chromatin contacts on its own,
299 but rather acts to stabilise or reinforce contacts already established between the two *Fab-7*
300 elements.

301

302 **Altered epigenetic states remain stable in the absence of artificially-induced chromatin** 303 **contacts**

304 These results demonstrate a clear role for chromatin contacts in the initial triggering of TEI in
305 Fab2L. However, due to experimental constraints, the 3D-CIS system remains active throughout
306 the selection towards epilines. To determine whether the altered epigenetic states triggered by
307 the 3D-CIS system can be maintained even in the absence of induced chromatin contacts, we
308 crossed the 3D-CIS epilines with a naïve LacO-Fab2L. In the F2, flies lacking the TetR-LacI
309 fusion protein (as determined by a GFP marker, see Methods) were selected and counted. Even
310 in the absence of the TetR-LacI inducing chromatin contacts, this F2 generation had a majority
311 of individuals with primarily white eyes, in the case of the white epiline (Figure 5K), or primarily
312 red eyes, in the case of the red epilines (Figure S11A). The distribution of the population was
313 comparable with those derived from a cross with Fab2L epilines triggered by transient
314 hemizygoty rather than 3D-CIS (Figure S11B,C). The LacO-Fab2L was therefore able to
315 maintain the memory of its altered epigenetic state, even in the absence of artificially-induced
316 chromatin contacts with the endogenous *Fab-7*, demonstrating that enhancement of chromatin
317 contacts is required to establish, but not maintain, transgenerational epigenetic inheritance.

318

319 **Discussion**

320 **GAF-mediated chromatin contacts and PRC2-mediated epigenetic variability together** 321 **account for TEI at the Fab2L transgene**

322 Our results highlight the crucial role played by two subdomains of the *Fab-7* element in the
323 establishment of epigenetic variation at the Fab2L transgene, and the maintenance of its
324 memory across generations. These subdomains are an insulator and a PRE, which act through
325 the recruitment of the transcription factors GAF and Pho. Alone, one of these regions remains
326 sufficient to maintain a certain degree of variation and epigenetic memory at the Fab2L
327 transgene, albeit in a manner skewed towards de-repression. Mutation of all GAF and Pho sites
328 across both regions, however, completely abrogates all variation, demonstrating that at least
329 some binding of these proteins is essential (Figures 1-2).

330 Our findings suggest that the insulator and PRE cooperate to control epigenetic regulation of the
331 *Fab-7* element in two ways. The first is the recruitment of PRC2, which deposits H3K27me3 in a
332 stochastic manner, leading to the observed variable eye colour phenotype. The second is to
333 mediate long-range chromatin contacts between the two distant *Fab-7* elements in the genome.
334 However, mutation of these subdomains suggests that the PRE is the comparatively more
335 important of the two regions for PRC2 recruitment (and thus epigenetic variability) (Figure 1E),
336 while the insulator is much more involved in the establishment of chromatin contacts (Figure 4).
337 Nevertheless, both elements contribute to some extent to both aspects of Fab2L regulation.

338 The distribution of GAF and Pho binding sites between these subdomains suggests differing
339 roles for these proteins, in agreement with what is known of their function. Indeed, the majority
340 of GAF binding sites (6 out of 9) are located in the insulator, while the majority of Pho sites (3
341 out of 4) are in the PRE (Figure 1B). Based on these observations, we propose that GAF is the
342 primary mediator of chromatin contacts, whereas Pho is the primary recruiter of PRC2, and thus
343 responsible for the epigenetic variability at the Fab2L transgene. Together, these proteins thus
344 mediate the dual functions of the *Fab-7* element, both of which are essential to TEI in this model
345 system.

346

347 **PRC2-dependent epigenetic memory at the Fab2L locus**

348 Our results clearly point to a central role for chromatin contacts in the establishment of TEI at
349 Fab2L, but not in the inheritance of the alternative gene expression at Fab2L, as contacts are
350 not present in early development (Figure S6). PRC2-deposited H3K27me3 is thus the primary
351 epigenetic signal underpinning the variability at the Fab2L transgene and must be inherited by
352 another mechanism independent of chromatin contacts, either by direct inheritance or by
353 reconstruction in each generation based on an epigenetic memory maintained by some other
354 signal⁶.

355 Alternatively, it is worth considering that a combination of direct and indirect inheritance
356 mechanisms could serve to reinforce each other, providing a more stable epigenetic memory
357 that either pathway alone. Previous work in *Drosophila* has provided evidence of germline
358 inheritance of H3K27me3, arguing for its ability to be transmitted through gametogenesis at
359 least³⁵. Moreover, a recent study found that a DNA-binding protein, in this case CTCF, can
360 remain bound to chromatin through development and maintain an epigenetic memory through
361 this association²⁰. That this mechanism could extend to a complex like PRC2, which both binds
362 to and deposits H3K27me3, is an interesting prospect, as it has the potential to provide a
363 positive feedback loop to stabilise transgenerational H3K27me3. In this way, inheritance of
364 H3K27me3 both directly, by transmission through the germline, and indirectly, through a
365 memory of PRC2 binding, could provide redundancy and reinforcement to ensure a more
366 reliable inheritance of epigenetic memory. While our study is primarily concerned with explaining
367 how TEI is triggered at the Fab2L locus, future investigations into the mechanism by which this
368 epigenetic state is transmitted across generations will provide a more complete picture of this
369 instance of TEI.

370

371 **Chromatin contacts trigger PRC2-dependent TEI at the Fab2L locus**

372 Our results indicate that the primary mechanism for the triggering of TEI at the Fab2L transgene
373 is the promotion of physical contact within the nucleus between Fab2L and the endogenous
374 *Fab-7*. Increased contact frequency can either be induced by hemizyosity (Figure S2) –
375 probably because the remaining copy of *Fab-7* forms contacts more efficiently with its distant
376 homolog at another locus in the absence of its homologous allele – or in a synthetic manner,
377 such as in our transgenic 3D-CIS system (Figure 5). This demonstrates that chromatin contacts
378 can establish transgenerational epigenetic memory in the absence of any genetic perturbation.
379 Nevertheless, we note that this system is unable to mimic the effects of hemizyosity in the

380 absence of an adjacent *Fab-7* element (Figure S10). This is explained by the fact that Fab2L-
381 *Fab-7* contacts are already observed to a lesser extent in Fab2L ; + individuals, but are
382 increased in Fab2L ; *Fab7*/+ hemizygotes (Figure 4A). Thus, 3D-CIS acts to increase or
383 stabilise the contacts already occurring between the two loci, rather than driving the contacts *de*
384 *novo*.

385 As this trigger can lead to inheritance of epigenetic state in both directions (repression and de-
386 repression), any mechanism explaining how this trigger occurs must take into account this
387 plasticity. We therefore propose a model whereby stabilisation of Fab2L-*Fab-7* chromatin
388 contacts allows for the exchange of PRC2 between the endogenous and transgenic *Fab-7*
389 elements, thereby triggering an epigenetic memory that can be selected towards extremes over
390 generations (Figure 6). In this model, naïve Fab2L flies have stochastic recruitment of PRC2 to
391 the transgene by Pho, leading to a random mosaic eye colour pattern (Figure 6A). Chromatin
392 contacts are mediated by GAF, but in the absence of manipulation these contacts primarily
393 occur between homologous alleles, i.e. Fab2L to Fab2L or endogenous *Fab-7* to endogenous
394 *Fab-7* (Figure 6B). While interchromosomal contacts between Fab2L and *Fab-7* do occur, they
395 are transient and outcompeted by the preferential interaction between homologous alleles that
396 is common in dipteran species³⁶ (Figure 6C). Stabilisation of these contacts is achieved upon
397 *Fab-7* hemizyosity (Figure 6D), because the remaining endogenous *Fab-7*, having lost its
398 preferred interaction partner, is free to form more stable contacts with its imperfect transgenic
399 partner without being outcompeted by its homologous allele. This situation can be mimicked in a
400 homozygous state, and in the absence of genetic perturbation, thanks to the 3D-CIS transgenic
401 system, which artificially stimulates chromatin contacts between Fab2L and *Fab-7*, making them
402 interact preferentially with each other rather than with their homologous alleles (Figure 6E).
403 When these trans interactions are sufficiently stable, exchange of PRC2 can occur between the
404 PREs of the *Fab-7* elements. Pho sites within the PRE can act as either donors or acceptors of
405 PRC2, leading to small changes in expression of the transgenic *mini-white* reporter. The
406 memory of this expression is maintained across generations, meaning that over time, these
407 differences can be selected to extremes, leading to either fully repressed or fully de-repressed
408 transgene expression, and monochrome eye colour (Figure 6F).

409 A few aspects of this model are worth highlighting. First, it would predict that a Fab2L/+ ;
410 *Fab7*[1]/+ double hemizygote, in which both loci have lost their preferential interaction partner
411 on the homologue, should be an even more effective trigger of TEI than single hemizyosity.
412 While we have not examined this in detail, our different TEI triggering crosses support this, as

413 epilines derived from *Fab2L/+* ; *Fab7[1]/+* double hemizygotes tend to reach fixation faster than
414 those derived from *Fab2L* ; *Fab7[1]/+* single hemizygotes during selection (Figure S2). Second,
415 exchange of PRC2 binding between *Fab2L* alleles, rather than between *Fab2L* and *Fab-7*, could
416 also explain how paramutation is able to transfer epigenetic state, albeit imperfectly, between
417 homologous alleles in this line. Our model thus accounts for both the triggering of epiallelic
418 identity, and its horizontal transfer by paramutation.

419

420 **A broader role for hemizyosity and chromatin contacts in triggering TEI**

421 One major question in the field of epigenetic inheritance is how heritable epigenetic variability,
422 or epimutation, arises in the first place. Studies in plants suggest that heritable changes in DNA
423 methylation can occur apparently spontaneously in these organisms, leading to long-term
424 epigenetic differences between lines³⁷⁻³⁹. Recent studies in *Caenorhabditis elegans* have
425 extended these observations to metazoans and to RNA and chromatin-based epigenetic
426 changes^{40,41}. Other studies have sought to identify environmental triggers for TEI, directly linking
427 epigenetic variation to an external stress to which it is intended to respond^{2,42,43}. The final
428 prominent candidate for sources of epigenetic variation is genetic perturbation, different types of
429 which have been shown to trigger TEI in a variety of organisms^{15,16,44,45}.

430 In the *Drosophila* *Fab2L* line, this genetic perturbation takes the form of transient hemizyosity
431 of the endogenous *Fab-7* region for at least one generation. It is interesting to note that unlike
432 some cases of genetically-triggered TEI, in *Fab2L* the epigenetic memory is triggered and
433 maintained not at the locus which is perturbed (the endogenous *Fab-7*) but elsewhere in the
434 genome (the *Fab2L* transgene), testifying to the ability of trans-interactions to induce TEI. *Fab-7*
435 has been found to have a similar effect on other loci. Indeed, hemizyosity of *Fab-7* has been
436 shown to affect the expression of another PRE-containing gene in the distant Antennapedia
437 cluster, with a phenotype that persisted for several generations after restoration of *Fab-7*
438 homozygosity¹⁹. This raises the question of whether similar mechanisms could be acting to
439 trigger TEI at other loci in natural populations.

440 Recent sequencing of wild *Drosophila melanogaster* lines has revealed the incredible genomic
441 variation between populations of this single species. This includes numerous and large-scale
442 deletions, duplications and translocations across the genome⁴⁶. Mixing of two such genomically
443 disparate populations would lead to a number of hemizyosity or heterozygosity events, as well
444 as homology between very distant loci reminiscent of what is observed in *Fab2L*. Breeding in

445 the wild thus has the potential to lead to many instances of naturally occurring genetic
446 perturbation as potential triggers for TEI. Just as in *Fab2L*, it could be that establishment of TEI
447 might be possible only between certain regions which are already prone to contact each other.
448 In this respect, PRC2 targets may be particularly interesting candidates for naturally occurring
449 TEI. Indeed, as previously mentioned, many PRC2 targets are frequently clustered within the
450 nucleus in polycomb bodies, forming a large domain of silenced chromatin⁴⁷. Interestingly,
451 genes regulated in this manner are more likely to possess both an insulator region and a PRE,
452 just like *Fab-7*. Our study provides insight into the mechanisms by which this type of epimutation
453 could occur, but it is only by extending this insight to a broader context that we will be able to
454 determine the role of TEI in the phenotypic variation, and thus potentially adaptation, of natural
455 populations.

456

457 **Acknowledgements**

458 We thank Montpellier Resources Imaging facility as well as the *Drosophila* facility (both affiliated
459 to BioCampus University of Montpellier, CNRS, INSERM, Montpellier, France). We thank Yuki
460 Ogiyama for assistance with the cloning of the plasmids for *Drosophila* injection and Judith
461 Kassis for the gift of the anti-Pho antibody. M.F.-J. and G.S. were supported by the European
462 Research Council Advanced Grant 3DEpi with additional support for M. F.-J from the MSD
463 Avenir Foundation Grant GENE-IGH. F.B. and G.C. were supported by CNRS. Research in the
464 P.S. lab was supported by the John Fell Fund (Grant No 0011417). Research in the G.C.
465 laboratory was supported by grants from the European Research Council (Advanced Grant
466 3DEpi), the European CHROMDESIGN ITN project (Marie Skłodowska-Curie grant agreement
467 No 813327), the European E-RARE NEURO DISEASES grant “IMPACT”, by the Agence
468 Nationale de la Recherche (PLASMADIFF3D, grant N. ANR-18-CE15-0010, LIUVCHROM,
469 grant N. ANR-21-CE45-0011), by the Fondation ARC (EpiMM3D), by the MSD Avenir
470 Foundation ((Project GENE-IGH), and by the French National Cancer Institute (INCa, PIT-MM
471 grant N. INCA-PLBIO18-362).

472

473 **Author contributions**

474 M. F.-J. and G.C. conceived of and led the project. M. F.-J. designed and performed the
475 experiments. M. F.-J. and G.C. interpreted the data. M. F.-J., G.S. and F.B. performed the

476 *Drosophila* transgenerational selection experiments. M. F-J. composed the manuscript with
477 editorial input from G.C. and P.S. All authors reviewed and commented on the manuscript.

478

479 **Declaration of Interests**

480 The authors declare no competing interests.

481

482 **Figure Titles & Legends**

483 **Figure 1. Mutation of GAF and Pho binding sites decreases epigenetic variability of the**
484 **Fab2L transgene.**

485 **(A)** Schematic representation of the Fab2L transgene at its insertion site at cytological position
486 37B on chromosome 2, alongside the homologous *Fab-7* region on chromosome 3.

487 **(B)** Illustration of the *Fab-7* element with important subdomains and transcription factor binding
488 sites in wild-type and mutated versions of the Fab2L transgene.

489 **(C-F)** ChIP-qPCR assays performed in embryos of the indicated genotypes at regions within the
490 Fab2L transgene. Error bars represent +/- standard error from the mean (SEM) of three
491 independent repeats. Samples were normalised to engrailed as a positive control and compared
492 to wild-type Fab2L or between each other by the t-test (* $p < 0.05$, ** $p < 0.01$, n.s. = not significant).

493 **(G-J)** Phenotypic classification of eye colour in female and male adults of the indicated
494 genotypes. Flies were sorted into five classes on the basis of eye colour, representing the
495 number of pigmented ommatidia: Class 1 = 0% ; Class 2 = 1-10% ; Class 3 = 10-75% ; Class 4
496 = 75-99% ; Class 5 = 100%. See also **Figure S1**.

497

498 **Figure 2. Epigenetic inheritance of eye colour is abrogated in the absence of GAF and**
499 **Pho binding to the Fab2L transgene.**

500 **(A)** Crossing scheme for the triggering of TEI at wild-type and mutant versions of Fab2L, with
501 diagrammatic representation of the copy number of the *Fab-7* element on chromosomes 2 and
502 3. See also **Figure S2**.

503 **(B-E)** Results of selection for the most white-eyed flies in each generation beyond the F2 of the
504 crossing scheme. At top, curves represent the percentage of Class 5 females in the population
505 across generations. Error bars are +/- standard deviation (SD) of 3 independent repeats. At
506 bottom, pie charts represent the phenotypic distribution of the eye colour within the population in
507 the first and last generations of selection, sorted into five classes. See Also **Figure S3**.

508

509 **Figure 3. The insulator and PRE regions are required for Fab2L to acquire a repressed**
510 **epigenetic state through paramutation.**

511 **(A)** Illustration of the paramutation crossing scheme for the acquisition of a repressed epigenetic
512 state by a naive Fab2L allele from an established epiallele *in trans*. The presence of a *black[1]*
513 marker linked to Fab2L allows for the identification of F2 individuals carrying two copies of the
514 transgene from the naive parent (grey chromosomes) rather than from the epiline parent (blue
515 chromosomes). See also **Figure S4**.

516 **(B-F)** Paramutation crossing schemes and phenotypic distribution of the populations with the
517 indicated genotypes and epiline identities. Pie charts represent the phenotypic distribution of the
518 eye colour within the population sorted into five classes.

519

520 **Figure 4. Long-distance chromatin contacts between Fab2L and Fab-7 depend on the**
521 **functionality of the insulator region.**

522 **(A,D,F)** Violin plots representing the distribution of average distance between the 37B and 89E
523 regions surrounding the Fab2L transgene and endogenous *Fab-7*, respectively, as determined
524 by FISH in the indicated genotypes. Distances were measured in stage 14-15 embryos in T1 and
525 T2 segments. Distributions were compared using the t-test (* $p < 0.05$, ** $p < 0.01$, n.s. = not
526 significant).

527 **(B,C)** Illustrative micrographs of FISH in embryonic nuclei of the indicated genotypes. Nuclei are
528 stained with DAPI in blue, the 37B locus surrounding the Fab2L transgene is stained in red and
529 the 89E locus surrounding the endogenous *Fab-7* is stained in green. Scale bars represent 1
530 μm . See also **Figure S5**.

531 **(E,G)** Bar graphs representing the percentage of cells from the same FISH assays in which the
532 inter-loci distance was less than 1 μm .

533

534 **Figure 5. An *in vivo* synthetic biology system promotes interchromosomal contacts**
535 **between *Fab-7* elements and is sufficient to induce TEI without genetic perturbation.**

536 **(A-C)** Schematic representation of the 3D-CIS system. Arrays of Lac and Tet operons are
537 inserted next to the transgenic and endogenous *Fab-7* elements. Expression of a TetR-LacI
538 fusion protein binding to both arrays promotes contacts between the two loci. Illustrative
539 micrographs represent nuclei from embryos with the 3D-CIS system in the “OFF” or “ON” state
540 with FISH highlighting the regions surrounding the *Fab-7* elements. Nuclei are stained with DAPI
541 in blue, the 37B locus is stained in red and the 89E locus is stained in green. Scale bars
542 represent 1 μm . See also **Figures S7 and S8**.

543 **(D)** Violin plots representing the distance distributions of the 37B and 89E regions surrounding
544 the two *Fab-7* elements as determined by FISH in the indicated genotypes. Distances were
545 measured in stage 14-15 embryos in T1 and T2 segments. Distributions were compared using
546 the t-test (* $p < 0.05$, ** $p < 0.01$, n.s. = not significant).

547 **(E)** Bar graphs representing the percentage of cells from the same FISH assays in which the
548 inter-loci distance was less than 1 μm .

549 **(F,G)** Results of selection for the most white or red-eyed flies in each generation of 3D-CIS flies
550 in either the “OFF” or “ON” state. Curves represent the percentage of males of Class 1 or Class
551 4+5 in the population across generations. Error bars are +/- SD of 3 independent repeats. Pie
552 charts represent the phenotypic distribution of the eye colour within the population in the first and
553 last generations of selection, sorted into five classes. See also **Figures S9, S10**.

554 **(H-J)** ChIP-qPCR assays against H3K27me3 performed in embryos of the indicated genotypes
555 after at least 10 generations of selection towards white or red epiallele identity, at regions within
556 the *Fab2L* transgene. Error bars represent +/- SEM of three independent repeats. Samples were
557 normalised to engrailed as a positive control and compared to each other by the t-test (* $p < 0.05$,
558 ** $p < 0.01$, n.s. = not significant).

559 **(K)** Paramutation crossing scheme and phenotypic distribution of the populations with the
560 indicated genotypes and epilines identities. See also **Figure S11**.

561

562 **Figure 6. Model: Stabilisation of interchromosomal contacts triggers an epigenetic**
563 **memory of PRC2 binding.**

564 **(A)** The *Fab-7* element recruits PRC2 by Pho binding to its PRE, leading to stochastic silencing
565 of a *mini-white* transgene and a mosaic eye colour.

566 **(B)** This PRC2 recruitment is coupled with long-range chromatin contacts with other *Fab-7*
567 elements mediated by GAF through an insulator region.

568 **(C)** When more than one copy of *Fab-7* is present in the genome contacts can be initiated
569 between distant *Fab-7* elements, but these contacts are outcompeted by inter-allelic contacts
570 and remain transient.

571 **(D-E)** Stabilization of these contacts can be achieved through hemizyosity of one *Fab-7* copy
572 (D) or through synthetic biology tools (E). This stabilisation leads to exchange of PRC2 between
573 the PREs, resulting in either increased PRC2 association and silencing, or decreased PRC2
574 association and de-repression, and triggering an epigenetic memory of this altered association.

575 **(F)** Over generations these slight differences can be selected to extremes, resulting in either
576 very strong or very weak repression and strikingly different phenotypes.

577

578 **Methods**

579 **Fly stocks and culture**

580 Flies were raised in standard cornmeal yeast extract media. Standard temperature was 21°C,
581 with the exception of P0 and F1 crosses in the experiments of Fab2L epiallele establishment by
582 hemizyosity or 3D-CIS (Figures 2; 5F,G; S2; S7A-D, S9D,E and S10D-I), for which temperature
583 was 18°C. The Fab2L and Fab2L ; *Fab7[1]* lines were described in Bantignies *et al.*, 2003²². The
584 Fab2L, *black[1]* line and pre-established Fab2L epilines (Fab2L-R* and Fab2L-W*) were
585 described in Ciabrelli *et al.*, 2017¹⁹.

586 For generation of the Fab2L mutant lines, a transgenic line was made containing an AttP
587 insertion site at cytogenetic position 37B, by CRISPR-Cas9 of a w[11118] line (Bloomington
588 Drosophila Stock Center) to cut at the exact site of Fab2L transgene insertion in the Fab2L line.
589 Fab2L-INS was then generated by Phi-recombination of an AttB-containing plasmid containing
590 the entirety of the Fab2L transgene, with directed mutations of the insulator GAF and Pho sites,
591 into this 37B-AttP line. Injection services for these two lines were provided by BestGene Inc..

592 Fab2L-PRE and Fab2L-INS-PRE were then generated by CRISPR-Cas9 editing of Fab2L-INS,
593 with a two-guide RNA strategy designed and implemented by Rainbowgene Transgenic Flies
594 Inc.

595 To create the 3D-CIS system, arrays of 7 Tet operators and 21 Lac operators were inserted
596 adjacent to the endogenous or transgenic *Fab-7*, respectively, using a single guide RNA to cut
597 immediately to their 3'. Cassettes encoding recombinant proteins combining the Lac and/or Tet
598 repressors with a GFP marker (TetR-GFP-LacI, TetR-GFP-TetR and LacI-GFP-LacI) under
599 expression of an *Actin-5C* promoter were inserted into chromosome arm 3L separately by Phi
600 recombination into an established AttP containing line (Bloomington 24480). The transgenes
601 encoding these proteins were then recombined with the TetO-*Fab-7*, and introduced into a
602 Fab2L background, ready to be crossed with the LacO-Fab2L as described in Supplementary
603 information, Figure S7. All injections for these lines were provided by BestGene Inc. The Fab2L-
604 *Fab-7* Δ line was derived from the LacO-Fab2L line by CRISPR-Cas9 targeted deletion of the
605 transgenic *Fab-7*, designed and implemented by Rainbowgene Transgenic Flies Inc.

606 Fab2L-INS, *black[1]*, Fab2L-PRE, *black[1]*, Fab2L-INS-PRE, *black[1]* and Fab2L-Fab7 Δ , *black[1]*
607 were generated by recombining the Fab2L transgene with the *black[1]* allele from the w[1118];
608 *black[1]* line (Bloomington Drosophila Stock Center).

609

610 **Chromatin Immunoprecipitation and antibodies**

611 0 to 16 hour old embryos were collected in Embryo Wash Buffer (0.03% Triton X-100, 140mM
612 NaCl) and dechorionated with bleach. Samples were crosslinked in 1 ml A1 buffer (60 mM KCl,
613 15 mM NaCl, 15 mM HEPES [pH 7.6], 4 mM MgCl₂, 0.5% Triton X-100, 0.5 mM dithiothreitol
614 (DTT), 10 mM sodium butyrate and complete EDTA-free protease inhibitor cocktail [Roche]), in
615 the presence of 1.8% formaldehyde. Samples were homogenized with a micropestle and
616 incubated for a total time of 15 minutes at room temperature. Crosslinking was stopped by
617 adding 350 mM glycine followed by incubation for 5 min. The homogenate was transferred to a 2
618 ml tube and centrifuged for 5 minutes, 4,000g at 4°C. The supernatant was discarded, and the
619 nuclear pellet was washed three times in 2 ml A1 buffer and once in 2 ml of Lysis buffer (140
620 mM NaCl, 15 mM HEPES [pH 7.6], 1 mM EDTA, 0.5mM EGTA, 1%Triton X-100, 0.5mMDTT,
621 0.1% sodium deoxycholate, 10 mM sodium butyrate and complete EDTA-free protease inhibitor
622 cocktail [Roche]) at 4°C. Nuclei were then resuspended in 1.5 ml Lysis buffer in the presence of
623 0.1% SDS and 0.5% N-Lauroylsarcosine, transferred to a 15 ml falcon tube and incubated for 2

624 hours with agitation at 4°C. Samples were adjusted to 3 ml and chromatin was sonicated using a
625 Q700 sonicator with microtip (QSonica) for a total of 6 minutes and 30 seconds at amplitude 50
626 (settings: 30 s on, 1min 30 s off x 13 cycles) in an ice bucket. Sheared chromatin had size range
627 of 100 to 300 base pairs. After sonication and 5 minutes high-speed centrifugation at 4°C,
628 fragmented chromatin was recovered in the supernatant and aliquoted in 5 µg (for H3K27me3
629 ChIP) or 20 µg (for non-histone protein ChIP) aliquots adjusted to a volume of 500 µl in Lysis
630 Buffer with 0.1% SDS and 0.5% N-Laurosylsarcosine for storage at -20°C.

631 To perform the ChIP, samples were thawed on ice and chromatin was precleared by addition of
632 15 µl of Protein A Dynabeads (Invitrogen 10002D) followed by incubation for at least 1 hour at
633 4°C. Dynabeads were removed on a magnetic rack and antibodies were added at a dilution of
634 1:100 (a mock control in the presence of rabbit IgG was performed at the same time, while an
635 input of the same size was set aside). Samples were incubated for overnight at 4°C on a rotating
636 wheel. 30 µl of Protein A Dynabeads were added and incubation was continued for at least 2
637 hours at 4°C. Antibody-protein complexes bound to beads were washed 4 times in Lysis Buffer
638 with 0.05% SDS and twice in TE Buffer (0.1 mM EDTA, 10 mM Tris (pH 8)) in 1 ml each time.
639 Chromatin was eluted from beads in 100 µl of 10 mM EDTA, 1% SDS, 50 mM Tris (pH 8) at
640 65°C for 15 minutes and eluted again in 150 µl of 10 mM EDTA, 0.67% SDS, 50 mM Tris (pH 8)
641 at 65°C for 15 minutes, with the eluate collected on a magnetic rack each time. The 250 µl
642 eluates and 250 µl of the Input DNA samples (1:2 input) were incubated overnight at 65°C to
643 reverse crosslinks and treated with Proteinase K for 3 hours at 56°C. DNA was isolated by
644 addition of an equal volume of phenol-chloroform, supernatants collected and then ethanol
645 precipitated for 2 hours at -20°C in the presence of 20 µg glycogen by addition of 25 µl 3M
646 sodium acetate and 625 µl ethanol. Samples were centrifuged at high speed for 1 hour and
647 washed in 500 µl of 70% ethanol before resuspension in 200 µl H₂O. Immunoprecipitated DNA
648 was used to analyze the enrichment of specific DNA fragments by real-time PCR (qPCR), using
649 a Roche Light Cycler 480 and the Light Cycler 480 SYBR green I Master mix. For each
650 amplicon, IP DNA was normalized to Input DNA. The ChIP/Input ratio was further normalized to
651 a positive control region (engrailed). ChIP amplicons for the insulator or PRE regions were
652 specific to either the WT or mutated transgenic sequence, depending on the genotype analysed.
653 Antibodies used in this study were as follows: anti-GAF polyclonal antibody⁴⁸; anti-Pho
654 polyclonal antibody^{48,49}; anti-E(z) polyclonal antibody³¹; anti-H3K27me3 polyclonal antibody
655 (Active Motif 39155), anti-GFP polyclonal antibody (Abcam ab290), normal rabbit IgG (Cell
656 Signalling 2729).

657 **Fluorescence in situ hybridization**

658 Two-color 3D FISH was performed as previously described⁵⁰. For a detailed protocol, see
659 Bantignies and Cavalli, 2014⁵¹. Briefly, embryos were dechorionated with bleach and fixed in
660 buffer A (60 mM KCl; 15 mM NaCl; 0.5 mM spermidine; 0.15 mM spermine; 2 mM EDTA; 0.5
661 mM EGTA; 15 mM PIPES, pH 7.4) with 4% paraformaldehyde for 25 min in the presence of
662 heptane. Embryos were then devitellinized by adding methanol to the heptane phase, extracted
663 and washed three times in methanol. Embryos were kept for a maximum of 4 months in
664 methanol at 4C before proceeding to FISH. Fixed embryos were sequentially re-hydrated in PBT
665 (PBS, 0.1% Tween 20) before being treated with 100–200 µg/ml RNaseA in PBT for 2 hours at
666 room temperature. Embryos were then sequentially transferred into a pre-Hybridization Mixture
667 (pHM: 50% formamide; 4XSSC; 100 mM NaH₂PO₄, pH 7.0; 0.1% Tween 20). Embryonic DNA
668 was denatured in pHM at 80°C for 15 minutes. The pHM was removed, and denatured probes
669 diluted in the FISH Hybridization Buffer (FHB: 10% dextransulfat; 50% deionized formamide;
670 2XSSC; 0.5 mg/ml Salmon Sperm DNA) were added to the tissues without prior cooling.
671 Hybridization was performed at 37°C overnight with gentle agitation. Post-hybridization washes
672 were performed, starting with 50% formamide, 2XSSC, 0.3% CHAPS and sequentially returning
673 to PBT. After an additional wash in PBS-Tr, DNA was counterstained with DAPI (at a final
674 concentration of 0.1 ng/µl) in PBT and embryos were mounted with ProLong Gold Antifade
675 (Invitrogen).

676 FISH probes for the 37B and 89E regions were made from a previous design described in
677 Ciabrelli et al. 2017¹⁹. For each region, 6 non-overlapping probes of between 1.2 and 1.7kb
678 covering an area of approximately 12kb were generated using the FISH Tag DNA kit with Alexa
679 Fluor 555 or Alexa Fluor 647 dyes (Invitrogen Life Technologies). 100ng of each probe were
680 added to the 30µL of FHB for hybridization.

681

682 **Microscopy and image analysis**

683 For the FISH, the 3D distances between 37B and 89E loci were acquired and measured as
684 follows: due to somatic pairing of homologous chromosomes in *Drosophila*, the majority of the
685 nuclei in embryos show a single FISH spot for each probe. In the cases of non-overlap FISH
686 signals between homologues, the closest distance between the centres of the two probes was
687 considered. To measure distances, 3D stacks were collected from 3-5 different embryos.

688 Optical sections were collected at 0.5 µm intervals along Z-axis using a Leica SP8-UV

689 microscope, Montpellier Resources Imaging (MRI) facility. Relative 3D distances between FISH
690 signals were analyzed in approximately 80 to 120 nuclei per 3D stack using the Imaris software
691 (Oxford Instruments). The distance distribution between the two probes was obtained by pooling
692 replicates for each condition.

693

694 **Supplemental Information Titles & Legends**

695 **Figure S1. Mutation of GAF and Pho sites leads to stronger red eye colour phenotypes.**

696 **(A-H)** Images showing randomly selected samples of 10 females and males of the indicated
697 genotypes.

698

699 **Figure S2. Transient hemizyosity of *Fab-7* triggers transgenerational epigenetic** 700 **inheritance at the *Fab2L* transgene.**

701 **(A-J)** Crossing schemes and results of subsequent selection towards epialles of the *Fab2L*
702 transgene. Selection was performed after either no cross (A,B), transient hemizyosity of the
703 endogenous *Fab-7* element (C,D), or transient hemizyosity of both the endogenous and
704 transgenic *Fab-7* elements, achieved from crosses with different parental genotypes (E-J). In
705 each case, *Fab2L* ; + flies derived from the indicated cross were split into two independent lines
706 and subjected to repeated selection of the most extreme white or red-eyed flies, respectively, in
707 each generation. Curves represent the percentage of Class 1 or Class 5 males in the population
708 across generations. Pie charts represent the phenotypic distribution of the eye colour within the
709 population in the first and last generations of selection.

710

711 **Figure S3. Epigenetic inheritance in males is abrogated in the absence of GAF and Pho** 712 **binding to the *Fab2L* transgene.**

713 **(A-D)** Results of selection for the most white-eyed flies in each generation beyond the F2 of the
714 crossing scheme. At top, curves represent the percentage of Class 5 males in the population
715 across generations. Error bars are +/- standard deviation (SD) of 3 independent repeats. At
716 bottom, pie charts represent the phenotypic distribution of the eye colour within the population in
717 the first and last generations of selection, separated into five classes.

718

719 **Figure S4. Fab2L can acquire a derepressed epigenetic state *in trans* by paramutation.**

720 **(A)** Illustration of the paramutation crossing scheme for the acquisition of a derepressed
721 epigenetic state by a naive Fab2L allele from an established epiallele *in trans*.

722 **(B)** Paramutation crossing scheme and phenotypic distribution of the populations with the
723 indicated genotypes and epiline identities. Pie charts represent the phenotypic distribution of the
724 eye colour within the population separated into five classes.

725

726 **Figure S5. Long-distance chromatin contacts between Fab2L and *Fab-7* increase upon
727 *Fab-7* hemizyosity, but not in insulator mutants.**

728 **(A-H)** Micrograph galleries of randomly selected nuclei of the indicated genotypes in FISH-
729 stained embryos. Nuclei are stained with DAPI in grey, the 37B locus surrounding the Fab2L
730 transgene is stained in blue and the 89E locus surrounding the endogenous *Fab-7* is stained in
731 green. Scale bar represents 1 μ m. The quantification associated with these images is
732 represented in **Figure 4**.

733

734 **Figure S6. Chromatin contacts between *Fab-7* elements are not present in the early
735 embryo.**

736 **(A)** Violin plots representing the distance distributions of the 37B and 89E regions surrounding
737 the two *Fab-7* elements as determined by FISH in the indicated genotypes and embryo stages.
738 Distributions were compared using the t-test (* $p < 0.05$, ** $p < 0.01$, n.s. = not significant).

739

740 **Figure S7. Synthetic constructs of the 3D-CIS system and its variants bind to their target
741 sequences.**

742 **(A-D)** Crossing schemes used to generate the 3D-CIS lines and associated controls.
743 Chromosomes 2 and 3 for each genotype of the crosses are illustrated with the different versions
744 of the *Fab-7* element highlighted. Red bars indicate a wild-type *Fab-7* at either the endogenous
745 (chromosome 3) or transgenic Fab2L (chromosome 2) locus. Purple and orange bars indicate

746 the array-containing LacO-Fab2L and TetO-Fab7, respectively. As illustrated, none of the
747 crosses introduce hemizyosity of either *Fab-7* element at any point.

748 **(E,F)** ChIP-qPCR assays in embryos of the indicated genotypes against LacI-TetR, TetR-TetR or
749 LacI-LacI using a GFP tag. Approximate positions of the loci analysed by each primer pair within
750 or adjacent to the *Fab-7* elements are indicated.

751

752 **Figure S8. Activation of the 3D-CIS system induces chromatin contacts between Fab2L**
753 **and *Fab-7*.**

754 **(A,B)** Micrograph galleries of randomly selected nuclei of the indicated genotypes in FISH-
755 stained embryos. Nuclei are stained with DAPI in grey, the 37B locus surrounding the Fab2L
756 transgene is stained in blue and the 89E locus surrounding the endogenous *Fab-7* is stained in
757 green. Scale bar represents 1 μ m. The quantification associated with these images is
758 represented in **Figure 5**.

759

760 **Figure S9. Promotion of chromatin contacts between homologous *Fab-7* alleles, rather**
761 **than interchromosomal loci, using the 3D-CIS system does not lead to TEI establishment.**

762 **(A-C)** Schematic representation of the 3D-CIS Tet and 3D-CIS Lac systems, variations on the
763 3D-CIS, used as controls. Arrays of Lac and Tet operons are inserted next to the transgenic and
764 endogenous *Fab-7* elements. Expression of a TetR-TetR or LacI-LacI fusion protein binding to
765 only one array controls for the potential induction of contacts between homologous alleles rather
766 than interchromosomal loci.

767 **(D,E)** Results of selection for the most white or red-eyed flies in each generation of 3D-CIS Tet
768 and 3D-CIS Lac flies in the “ON” state. Curves represent the percentage of males of Class 1 or
769 Class 4+5 in the population across generations. Error bars are +/- SD of 3 independent repeats.
770 Pie charts represent the phenotypic distribution of the eye colour within the population in the first
771 and last generations of selection.

772 **(F,G)** ChIP-qPCR assays against H3K27me3 performed in embryos of the indicated genotypes
773 after selection towards white or red epiallele identity, at regions within the Fab2L transgene.
774 Error bars represent +/- SEM of three independent repeats. Samples were normalised to

775 engrailed as a positive control and compared to each other by the t-test (* $p < 0.05$, ** $p < 0.01$, n.s.
776 = not significant).

777

778 **Figure S10. Artificial promotion of chromatin contacts is unable to significantly decrease**
779 **inter-loci distance or trigger TEI in the absence of the *Fab-7* element.**

780 **(A,F,H)** Schematic representation of the 3D-CIS-*Fab7* Δ line in which the *Fab-7* element was
781 deleted from the *Fab2L* transgene of the 3D-CIS line.

782 **(B)** Phenotypic classification of eye colour of the 3D-CIS-*Fab7* Δ flies.

783 **(C)** Paramutation crossing scheme and phenotypic distribution of the populations with the
784 indicated genotypes and epiline identities.

785 **(D)** Crossing scheme for the triggering of TEI in *Fab2L-Fab7* Δ , with diagrammatic representation
786 of the copy number of the *Fab-7* element on chromosomes 2 and 3.

787 **(E,G,I)** Results of selection for the most white-eyed flies in each generation after the cross or in
788 the 3D-CIS system. Curves represent the percentage of Class 5 males in the population across
789 generations. Error bars are +/- standard deviation (SD) of 3 independent repeats.

790 **(J)** Violin plots representing the distance distributions of the 37B and 89E regions surrounding
791 the two *Fab-7* elements as determined by FISH in the indicated genotypes. Distances were
792 measured in stage 14-15 embryos in T1 and T2 segments. Distributions were compared using
793 the t-test (n.s. = not significant, i.e. $p > 0.05$).

794

795 **Figure S11. Altered epigenetic states remain stable in the absence of artificially-induced**
796 **chromatin contacts**

797 **(A-C)** Paramutation crossing schemes and phenotypic distribution of the populations with the
798 indicated genotypes and epiline identities. Pie charts represent the phenotypic distribution of the
799 eye colour within the population separated into five classes.

800

801

802 **References**

- 803 1. Allis, C.D., and Jenuwein, T. (2016). The molecular hallmarks of epigenetic control. *Nat.*
804 *Rev. Genet.* *17*, 487–500. 10.1038/nrg.2016.59.
- 805 2. Cavalli, G., and Heard, E. (2019). Advances in epigenetics link genetics to the
806 environment and disease. *Nature* *571*, 489–499. 10.1038/s41586-019-1411-0.
- 807 3. Bohacek, J., and Mansuy, I.M. (2017). A guide to designing germline-dependent
808 epigenetic inheritance experiments in mammals. *Nat. Methods* *14*, 243–249.
809 10.1038/nmeth.4181.
- 810 4. Liberman, N., Wang, S.Y., and Greer, E.L. (2019). Transgenerational Epigenetic
811 Inheritance: From Phenomena to Molecular Mechanisms. *Curr. Opin. Neurobiol.*
812 10.1016/j.conb.2019.09.012.
- 813 5. Bošković, A., and Rando, O.J. (2018). Transgenerational epigenetic inheritance. *Annu.*
814 *Rev. Genet.* *52*, 21–41. 10.1146/annurev-genet-120417-031404.
- 815 6. Fitz-James, M.H., and Cavalli, G. (2022). Molecular mechanisms of transgenerational
816 epigenetic inheritance. *Nat. Rev. Genet.* *23*, 325–341. 10.1038/s41576-021-00438-5.
- 817 7. Rechavi, O., Houry-Ze’Evi, L., Anava, S., Goh, W.S.S., Kerk, S.Y., Hannon, G.J., and
818 Hobert, O. (2014). Starvation-induced transgenerational inheritance of small RNAs in *C.*
819 *elegans*. *Cell* *158*, 277–287. 10.1016/j.cell.2014.06.020.
- 820 8. Schott, D., Yanai, I., and Hunter, C.P. (2015). Natural RNA interference directs a
821 heritable response to the environment. *Sci. Rep.* *4*, 7387. 10.1038/srep07387.
- 822 9. Teixeira, F.K., Okuniewska, M., Malone, C.D., Coux, R.X., Rio, D.C., and Lehmann, R.
823 (2017). PiRNA-mediated regulation of transposon alternative splicing in the soma and
824 germ line. *Nature* *552*, 268–272. 10.1038/nature25018.
- 825 10. Duempelmann, L., Skribbe, M., and Bühler, M. (2020). Small RNAs in the
826 Transgenerational Inheritance of Epigenetic Information. *Trends Genet.* *36*, 203–214.
827 10.1016/j.tig.2019.12.001.
- 828 11. Cecere, G. (2021). Small RNAs in epigenetic inheritance: from mechanisms to trait
829 transmission. *FEBS Lett.* *595*, 2953–2977. 10.1002/1873-3468.14210.
- 830 12. Yu, R., Wang, X., and Moazed, D. (2018). Epigenetic inheritance mediated by coupling of
831 RNAi and histone H3K9 methylation. *Nature* *558*, 615–619. 10.1038/s41586-018-0239-3.

- 832 13. Furci, L., Jain, R., Stassen, J., Berkowitz, O., Whelan, J., Roquis, D., Baillet, V., Colot, V.,
833 Johannes, F., and Ton, J. (2019). Identification and characterisation of hypomethylated
834 DNA loci controlling quantitative resistance in *Arabidopsis*. *Elife* 8, e40655.
835 10.7554/eLife.40655.
- 836 14. Silveira, A.B., Trontin, C., Cortijo, S., Barau, J., Del Bem, L.E.V., Loudet, O., Colot, V.,
837 and Vincentz, M. (2013). Extensive Natural Epigenetic Variation at a De Novo Originated
838 Gene. *PLoS Genet.* 9, e1003437. 10.1371/journal.pgen.1003437.
- 839 15. Takahashi, Y., Morales Valencia, M., Yu, Y., Ouchi, Y., Takahashi, K., Shokhirev, M.N.,
840 Lande, K., Williams, A.E., Fresia, C., Kurita, M., et al. (2023). Transgenerational
841 inheritance of acquired epigenetic signatures at CpG islands in mice. *Cell* 186, 715–731.
842 10.1016/j.cell.2022.12.047.
- 843 16. Greer, E.L., Maures, T.J., Ucar, D., Hauswirth, A.G., Mancini, E., Lim, J.P., Benayoun,
844 B.A., Shi, Y., and Brunet, A. (2011). Transgenerational epigenetic inheritance of longevity
845 in *Caenorhabditis elegans*. *Nature* 479, 365–371. 10.1038/nature10572.
- 846 17. Torres-Garcia, S., Yaseen, I., Shukla, M., Audergon, P.N.C.B., White, S.A., Pidoux, A.L.,
847 and Allshire, R.C. (2020). Epigenetic gene silencing by heterochromatin primes fungal
848 resistance. *Nature* 585, 453–458. 10.1038/s41586-020-2706-x.
- 849 18. Seong, K.H., Li, D., Shimizu, H., Nakamura, R., and Ishii, S. (2011). Inheritance of stress-
850 induced, ATF-2-dependent epigenetic change. *Cell* 145, 1049–1061.
851 10.1016/j.cell.2011.05.029.
- 852 19. Ciabrelli, F., Comoglio, F., Fellous, S., Bonev, B., Ninova, M., Szabo, Q., Xuéreb, A.,
853 Klopp, C., Aravin, A., Paro, R., et al. (2017). Stable Polycomb-dependent
854 transgenerational inheritance of chromatin states in *Drosophila*. *Nat. Genet.* 49, 876–886.
855 10.1038/ng.3848.
- 856 20. Jung, Y.H., Wang, H.-L. V., Ruiz, D., Bixler, B.J., Linsenbaum, H., Xiang, J.-F., Forestier,
857 S., Shafik, A.M., Jin, P., and Corces, V.G. (2022). Recruitment of CTCF to an *Fto*
858 enhancer is responsible for transgenerational inheritance of BPA-induced obesity. *Proc.*
859 *Natl. Acad. Sci.* 119. 10.1073/pnas.2214988119.
- 860 21. Sabarís, G., Fitz-James, M.H., and Cavalli, G. (2023). Epigenetic inheritance in adaptive
861 evolution. *Ann. N. Y. Acad. Sci.* 1524, 22–29. 10.1111/nyas.14992.

- 862 22. Bantignies, F., Grimaud, C., Lavrov, S., Gabut, M., and Cavalli, G. (2003). Inheritance of
863 polycomb-dependent chromosomal interactions in *Drosophila*. *Genes Dev.* *17*, 2406–
864 2420. [10.1101/gad.269503](https://doi.org/10.1101/gad.269503).
- 865 23. Zink, D., and Paro, R. (1995). *Drosophila* Polycomb-group regulated chromatin inhibits
866 the accessibility of a trans-activator to its target DNA. *EMBO J.* *14*, 5660–5671.
867 [10.1002/j.1460-2075.1995.tb00253.x](https://doi.org/10.1002/j.1460-2075.1995.tb00253.x).
- 868 24. Maeda, R.K., and Karch, F. (2006). The ABC of the BX-C: the bithorax complex
869 explained. *Development* *133*, 1413–1422. [10.1242/dev.02323](https://doi.org/10.1242/dev.02323).
- 870 25. Kyrchanova, O., Mogila, V., Wolle, D., Deshpande, G., Parshikov, A., Cléard, F., Karch,
871 F., Schedl, P., and Georgiev, P. (2016). Functional Dissection of the Blocking and Bypass
872 Activities of the Fab-8 Boundary in the *Drosophila* Bithorax Complex. *PLoS Genet.* *12*, 1–
873 22. [10.1371/journal.pgen.1006188](https://doi.org/10.1371/journal.pgen.1006188).
- 874 26. Kyrchanova, O., Sabirov, M., Mogila, V., Kurbidaeva, A., Postika, N., Maksimenko, O.,
875 Schedl, P., and Georgiev, P. (2019). Complete reconstitution of bypass and blocking
876 functions in a minimal artificial *Fab-7* insulator from *Drosophila bithorax* complex. *Proc.*
877 *Natl. Acad. Sci.*, 201907190. [10.1073/pnas.1907190116](https://doi.org/10.1073/pnas.1907190116).
- 878 27. Hollick, J.B. (2016). Paramutation and related phenomena in diverse species. *Nat. Rev.*
879 *Genet.* *18*, 5–23. [10.1038/nrg.2016.115](https://doi.org/10.1038/nrg.2016.115).
- 880 28. Dorer, D.R., and Henikoff, S. (1997). Transgene repeat arrays interact with distant
881 heterochromatin and cause silencing in cis and trans. *Genetics* *147*, 1181–1190.
882 [10.1093/genetics/147.3.1181](https://doi.org/10.1093/genetics/147.3.1181).
- 883 29. De Vanssay, A., Bougé, A.L., Boivin, A., Hermant, C., Teyssset, L., Delmarre, V.,
884 Antoniewski, C., and Ronsseray, S. (2012). Paramutation in *Drosophila* linked to
885 emergence of a piRNA-producing locus. *Nature* *490*, 112–115. [10.1038/nature11416](https://doi.org/10.1038/nature11416).
- 886 30. Capovilla, M., Robichon, A., and Rassoulzadegan, M. (2017). A new paramutation-like
887 example at the Delta gene of *Drosophila*. *PLoS One* *12*, 1–16.
888 [10.1371/journal.pone.0172780](https://doi.org/10.1371/journal.pone.0172780).
- 889 31. Ogiyama, Y., Schuettengruber, B., Papadopoulos, G.L., Chang, J.M., and Cavalli, G.
890 (2018). Polycomb-Dependent Chromatin Looping Contributes to Gene Silencing during
891 *Drosophila* Development. *Mol. Cell* *71*, 73-88.e5. [10.1016/j.molcel.2018.05.032](https://doi.org/10.1016/j.molcel.2018.05.032).

- 892 32. Mahmoudi, T., Katsani, K.R., and Verrijzer, C.P. (2002). GAGA can mediate enhancer
893 function in trans by linking two separate DNA molecules. *EMBO J.* 21, 1775–1781.
894 10.1093/emboj/21.7.1775.
- 895 33. Chetverina, D., Erokhin, M., and Schedl, P. (2021). GAGA factor – a multifunctional
896 pioneering chromatin protein. *Cell Mol. Life Sci.* 78, 4125–4141. 10.1007/s00018-021-
897 03776-z.
- 898 34. Entrevan, M., Schuettengruber, B., and Cavalli, G. (2016). Regulation of Genome
899 Architecture and Function by Polycomb Proteins. *Trends Cell Biol.* 26, 511–525.
900 10.1016/j.tcb.2016.04.009.
- 901 35. Zenk, F., Loeser, E., Schiavo, R., Kilpert, F., Bogdanović, O., and Iovino, N. (2017). Germ
902 line–inherited H3K27me3 restricts enhancer function during maternal-to-zygotic
903 transition. *Science* 357, 212–216. 10.1126/science.aam5339.
- 904 36. McKee, B.D. (2004). Homologous pairing and chromosome dynamics in meiosis and
905 mitosis. *Biochim. Biophys. Acta - Gene Struct. Expr.* 1677, 165–180.
906 10.1016/j.bbaexp.2003.11.017.
- 907 37. Johannes, F., and Schmitz, R.J. (2019). Spontaneous epimutations in plants. *New Phytol.*
908 221, 1253–1259. 10.1111/nph.15434.
- 909 38. Johannes, F., Porcher, E., Teixeira, F.K., Saliba-Colombani, V., Simon, M., Agier, N.,
910 Bulski, A., Albuissou, J., Heredia, F., Audigier, P., et al. (2009). Assessing the Impact of
911 Transgenerational Epigenetic Variation on Complex Traits. *PLoS Genet.* 5, e1000530.
912 10.1371/journal.pgen.1000530.
- 913 39. Kawakatsu, T., Huang, S. shan C., Jupe, F., Sasaki, E., Schmitz, R.J.J., Urich, M.A.A.,
914 Castanon, R., Nery, J.R.R., Barragan, C., He, Y., et al. (2016). Epigenomic Diversity in a
915 Global Collection of Arabidopsis thaliana Accessions. *Cell* 166, 492–505.
916 10.1016/j.cell.2016.06.044.
- 917 40. Beltran, T., Shahrezaei, V., Katju, V., and Sarkies, P. (2020). Epimutations driven by
918 small RNAs arise frequently but most have limited duration in *Caenorhabditis elegans*.
919 *Nat. Ecol. Evol.* 4, 1539–1548. 10.1038/s41559-020-01293-z.
- 920 41. Wilson, R., Le Bourgeois, M., Perez, M., and Sarkies, P. (2023). Fluctuations in
921 chromatin state at regulatory loci occur spontaneously under relaxed selection and are

- 922 associated with epigenetically inherited variation in *C. elegans* gene expression
923 10.1371/journal.pgen.1010647.
- 924 42. Klosin, A., Casas, E., Hidalgo-Carcedo, C., Vavouri, T., and Lehner, B. (2017).
925 Transgenerational transmission of environmental information in *C. elegans*. *Science* 356,
926 320–323. 10.1126/science.aah6412.
- 927 43. Casier, K., Boivin, A., Carré, C., and Teyssset, L. (2019). Environmentally-Induced
928 Transgenerational Epigenetic Inheritance: Implication of PIWI Interacting RNAs. *Cells* 8,
929 1108. 10.3390/cells8091108.
- 930 44. Reinders, a., Burckert, N., Boller, T., Wiemken, a., and De Virgilio, C. (1998).
931 *Saccharomyces cerevisiae* cAMP-dependent protein kinase controls entry into stationary
932 phase through the Rim15p protein kinase. *Genes Dev.* 12, 2943–2955.
933 10.1101/gad.12.18.2943.
- 934 45. Rassoulzadegan, M., Grandjean, V., Gounon, P., Vincent, S., Gillot, I., and Cuzin, F.
935 (2006). RNA-mediated non-mendelian inheritance of an epigenetic change in the mouse.
936 *Nature* 441, 469–474. 10.1038/nature04674.
- 937 46. MacKay, T.F.C., Richards, S., Stone, E.A., Barbadilla, A., Ayroles, J.F., Zhu, D., Casillas,
938 S., Han, Y., Magwire, M.M., Cridland, J.M., et al. (2012). The *Drosophila melanogaster*
939 Genetic Reference Panel. *Nature* 482, 173–178. 10.1038/nature10811.
- 940 47. Entrevan, M., Schuettengruber, B., and Cavalli, G. (2016). Regulation of Genome
941 Architecture and Function by Polycomb Proteins. *Trends Cell Biol.* 26, 511–525.
942 10.1016/j.tcb.2016.04.009.
- 943 48. Schuettengruber, B., Ganapathi, M., Leblanc, B., Portoso, M., Jaschek, R., Tolhuis, B.,
944 Van Lohuizen, M., Tanay, A., and Cavalli, G. (2009). Functional anatomy of polycomb
945 and trithorax chromatin landscapes in *Drosophila* embryos. *PLoS Biol.* 7.
946 10.1371/journal.pbio.1000013.
- 947 49. Brown, J.L., Fritsch, C., Mueller, J., and Kassis, J.A. (2003). The *Drosophila* *pho*-like
948 gene encodes a YY1-related DNA binding protein that is redundant with pleiohomeotic in
949 homeotic gene silencing. *Development* 130, 285–294. 10.1242/dev.00204.
- 950 50. Bantignies, F., Roure, V., Comet, I., Leblanc, B., Schuettengruber, B., Bonnet, J., Tixier,
951 V., Mas, A., and Cavalli, G. (2011). Polycomb-dependent regulatory contacts between

- 952 distant Hox loci in *Drosophila*. *Cell* *144*, 214–226. 10.1016/j.cell.2010.12.026.
- 953 51. Bantignies, F., and Cavalli, G. (2014). Topological Organization of *Drosophila* Hox Genes
954 Using DNA Fluorescent In Situ Hybridization. *Methods Mol. Biol.* *1196*, 103–120.
955 10.1007/978-1-4939-1242-1_7.
- 956

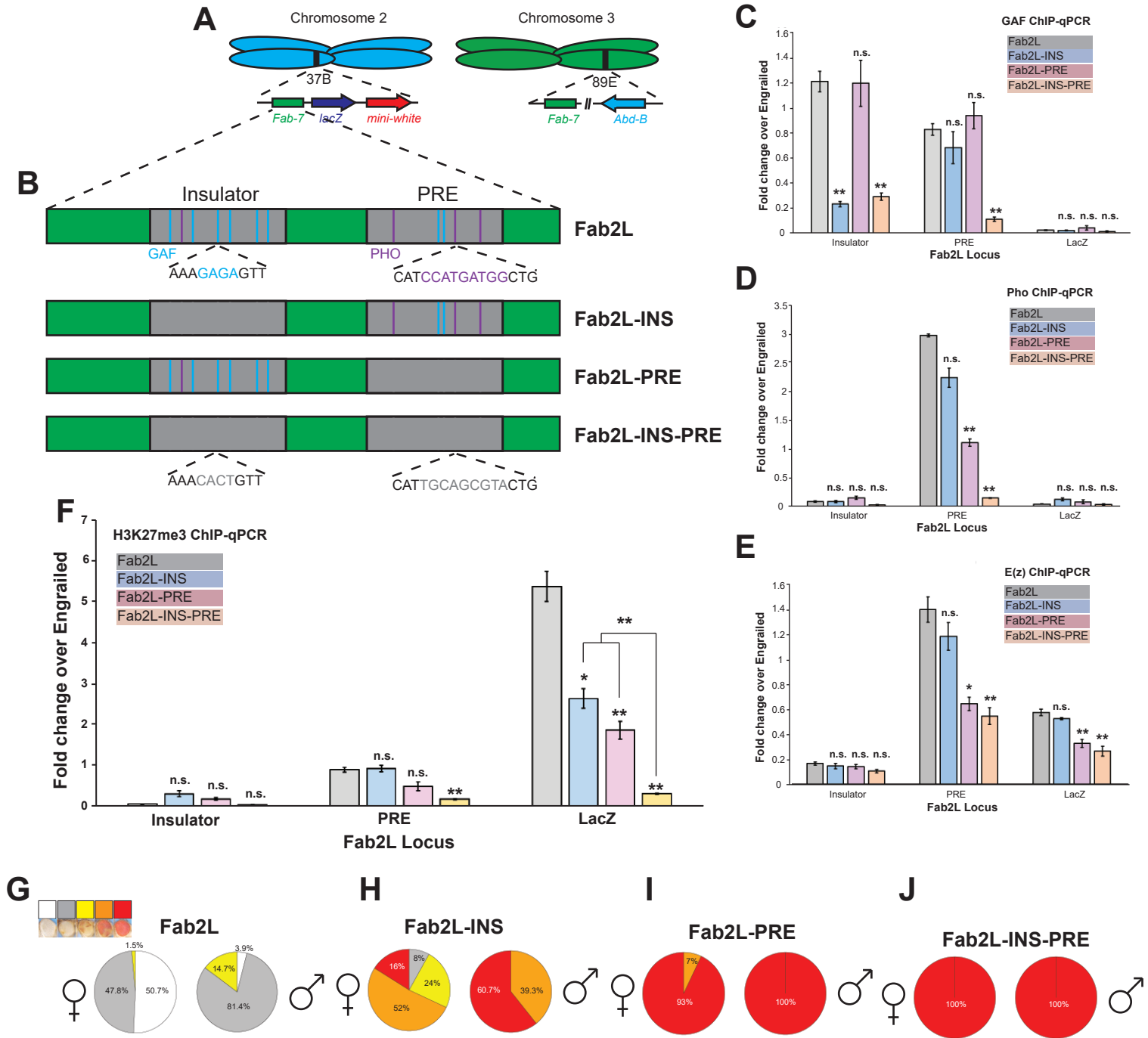


Figure 1

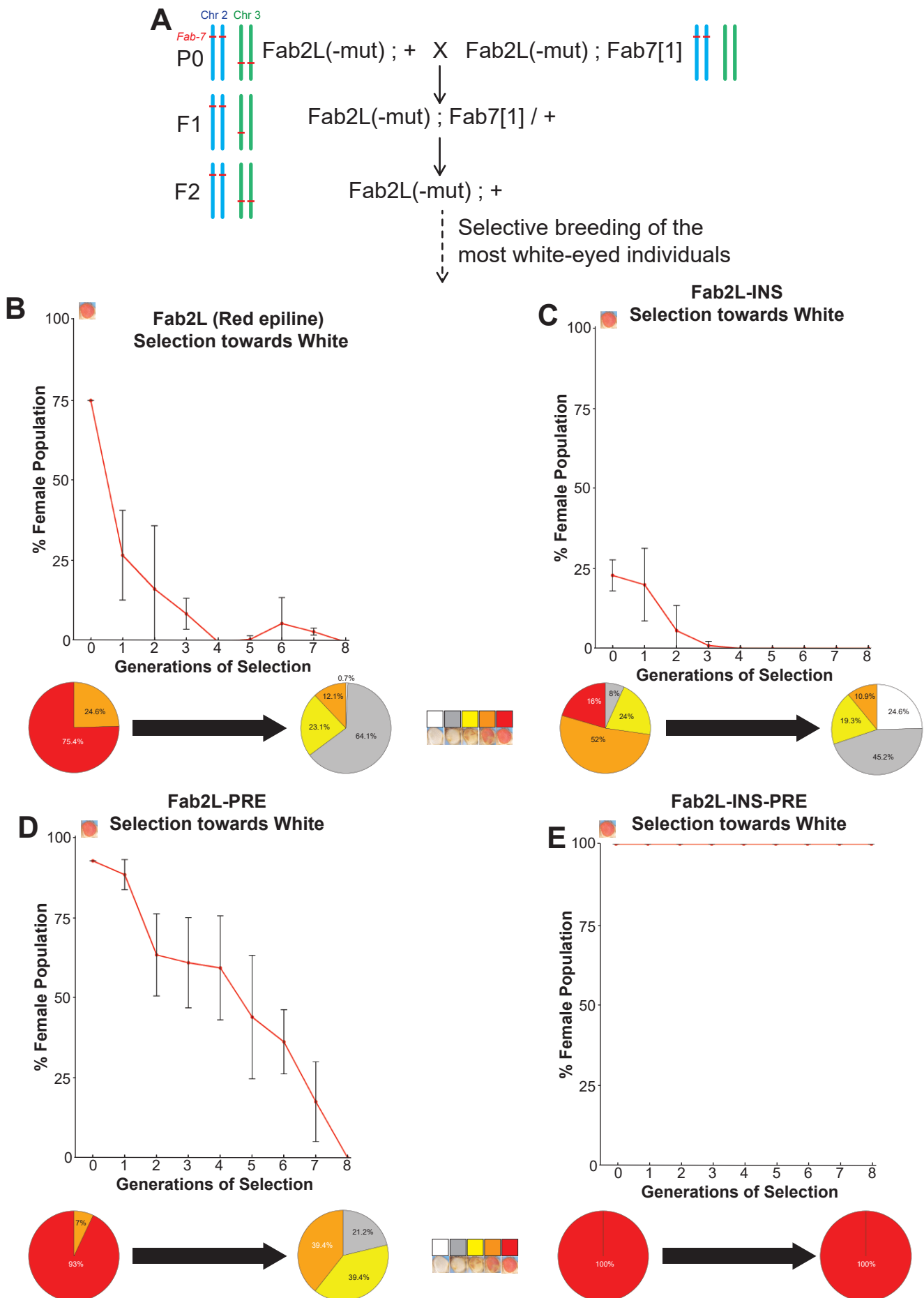


Figure 2

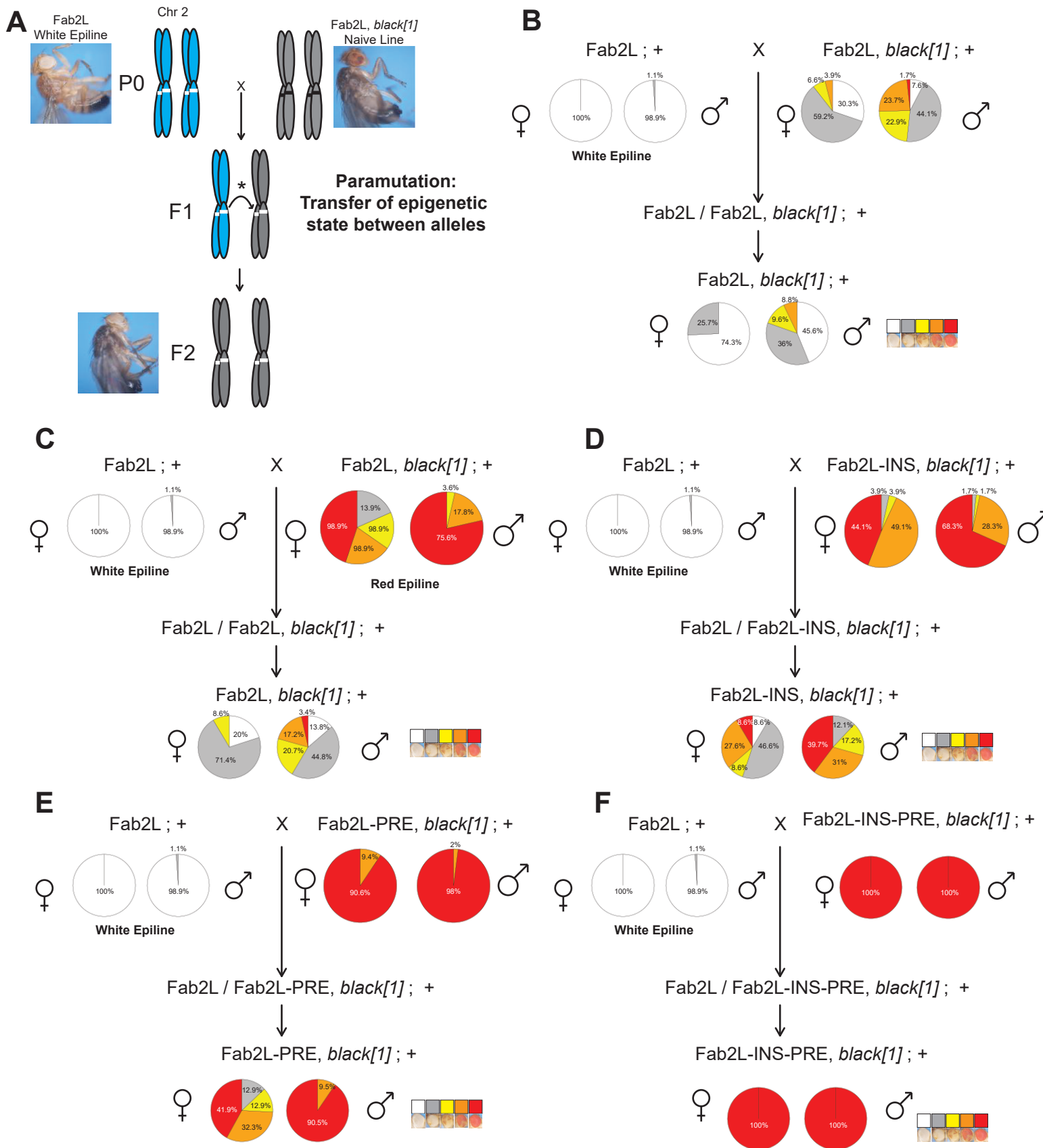


Figure 3

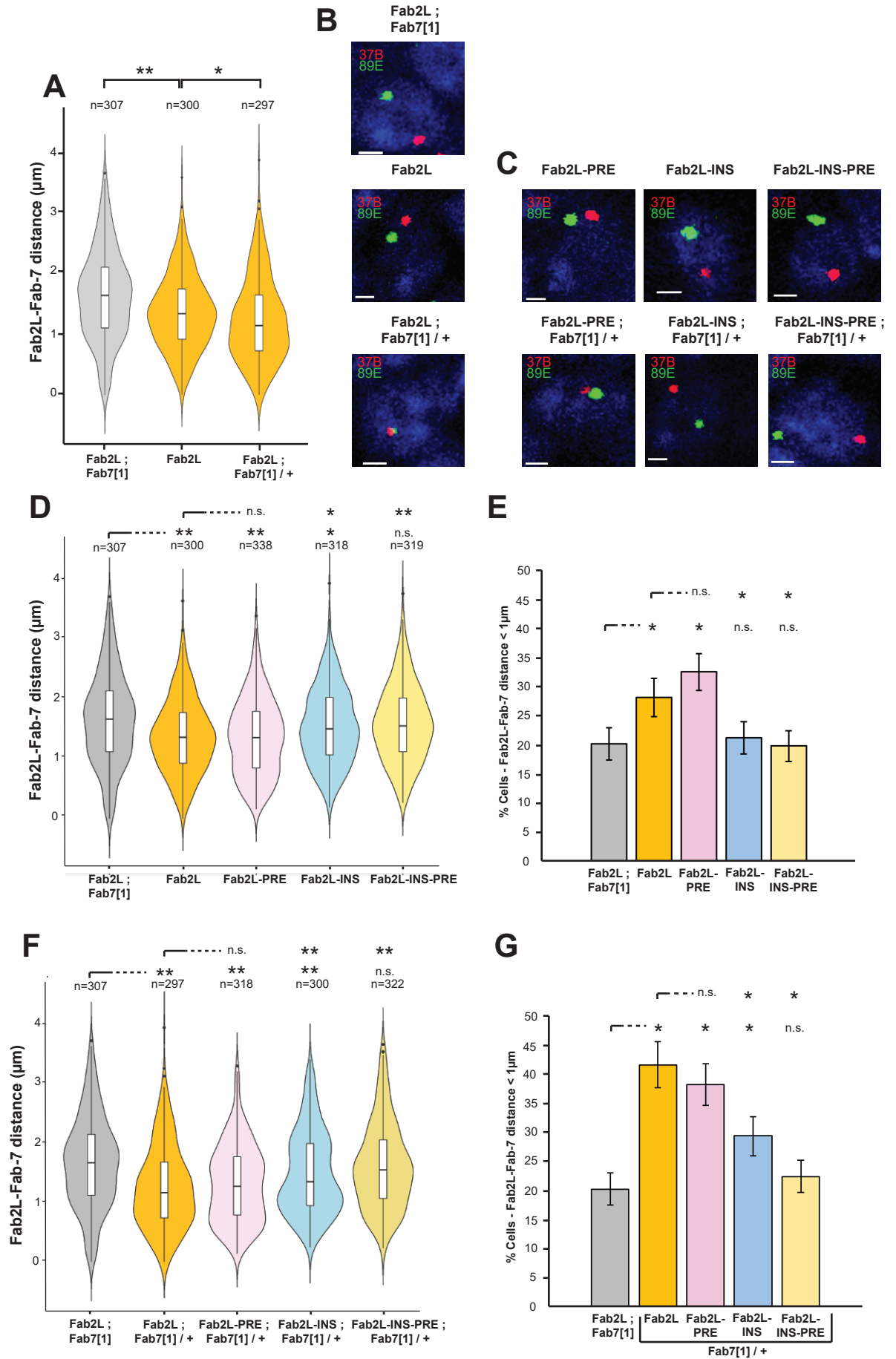


Figure 4

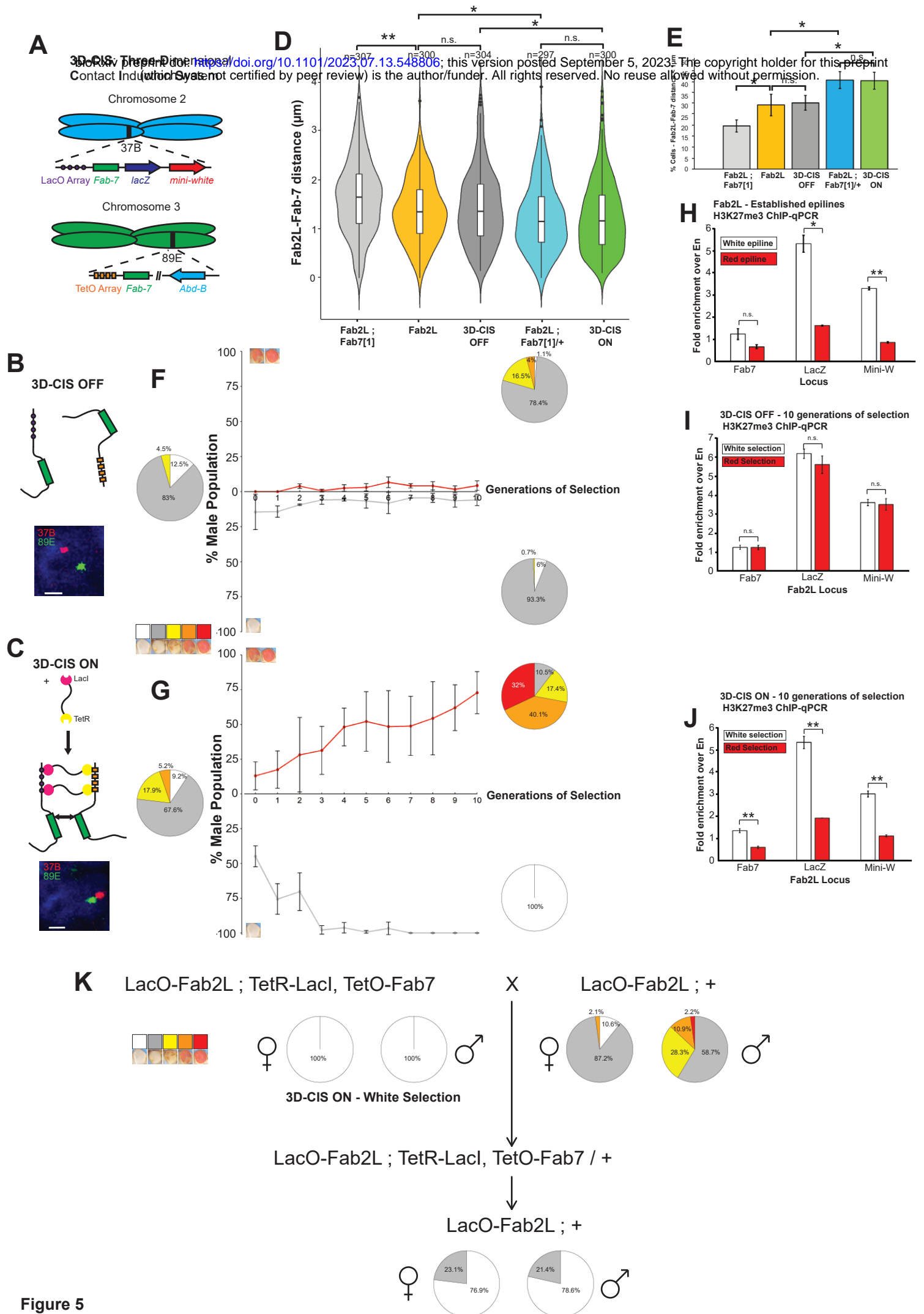


Figure 5

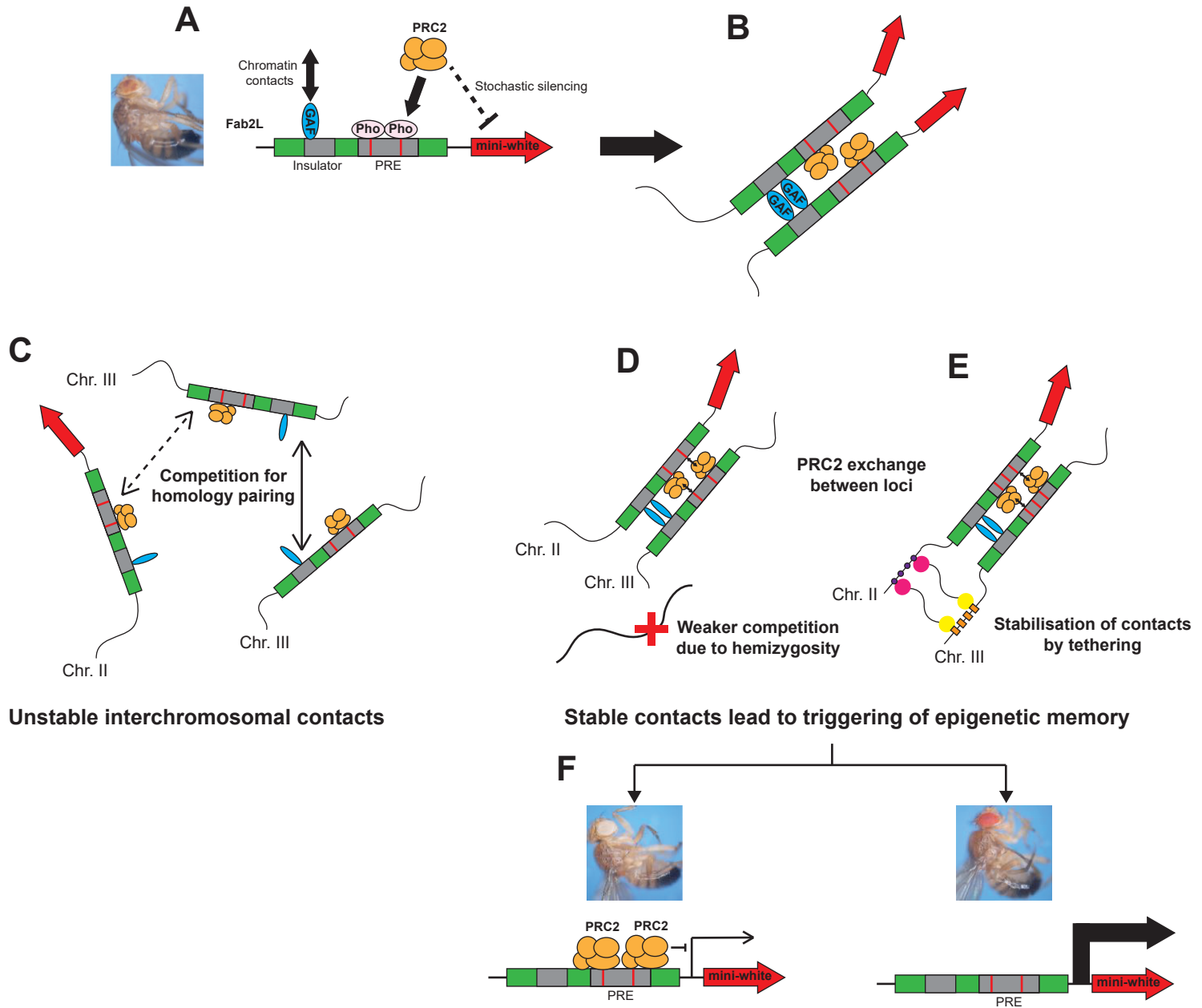


Figure 6

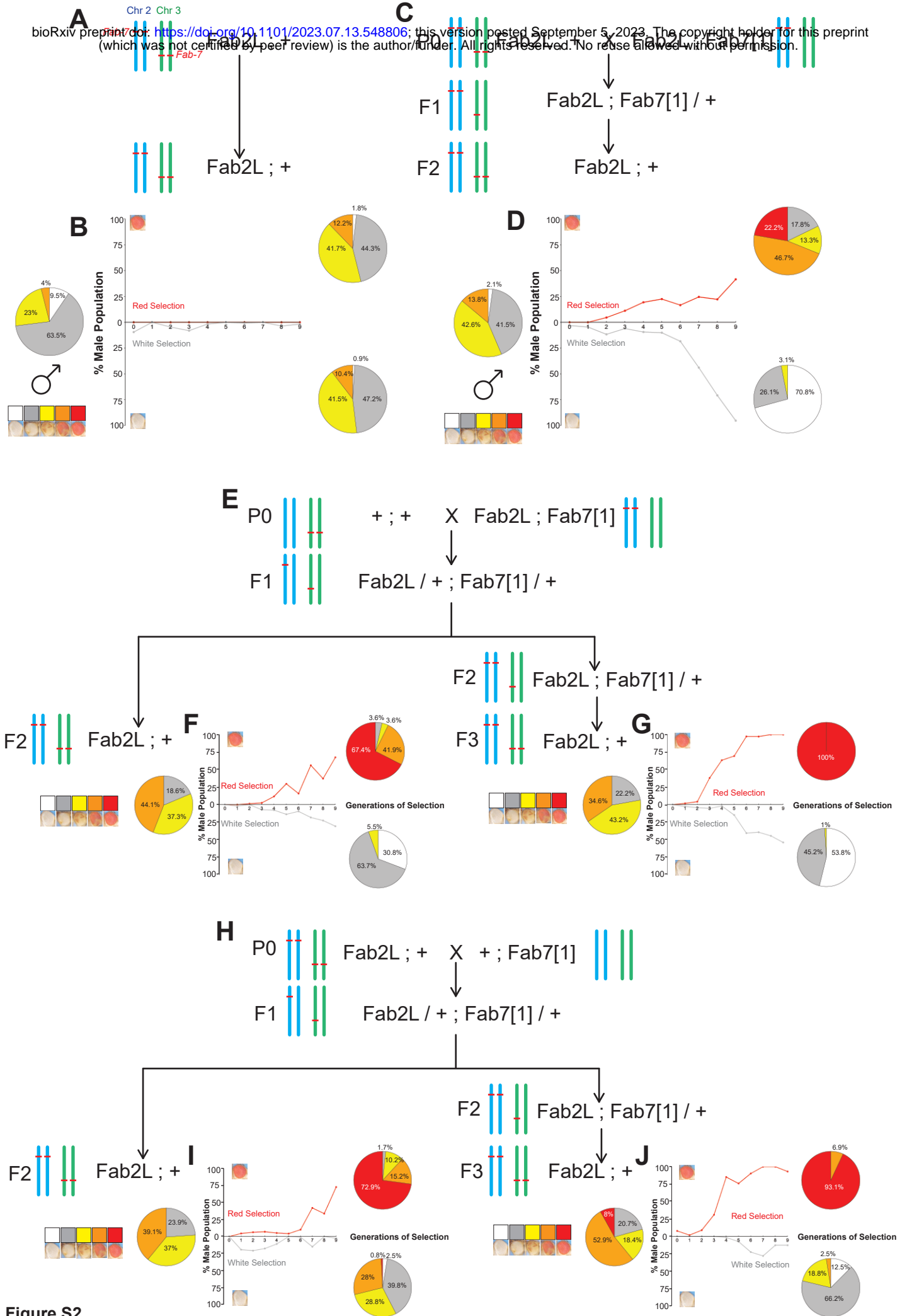


Figure S2

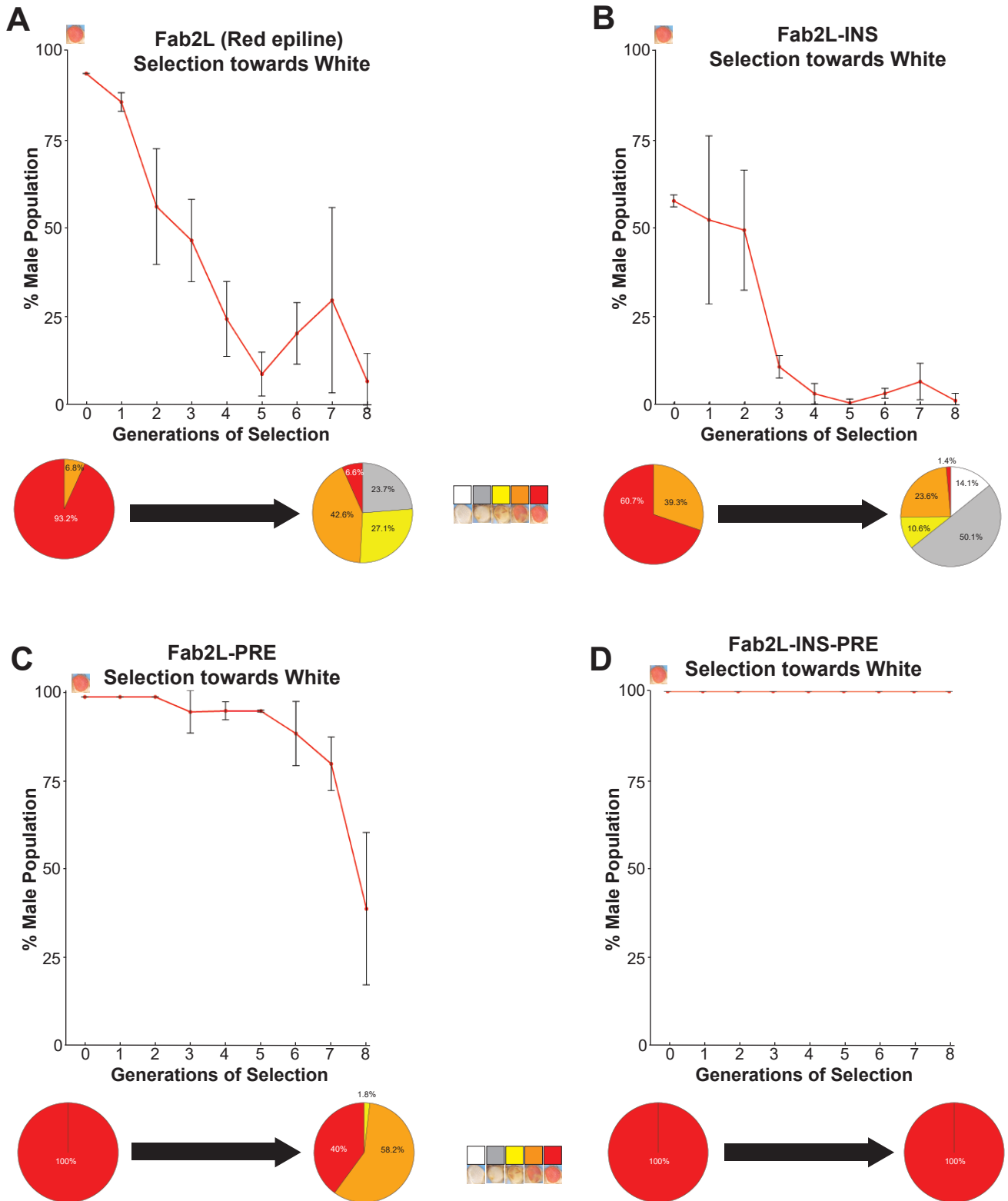


Figure S3

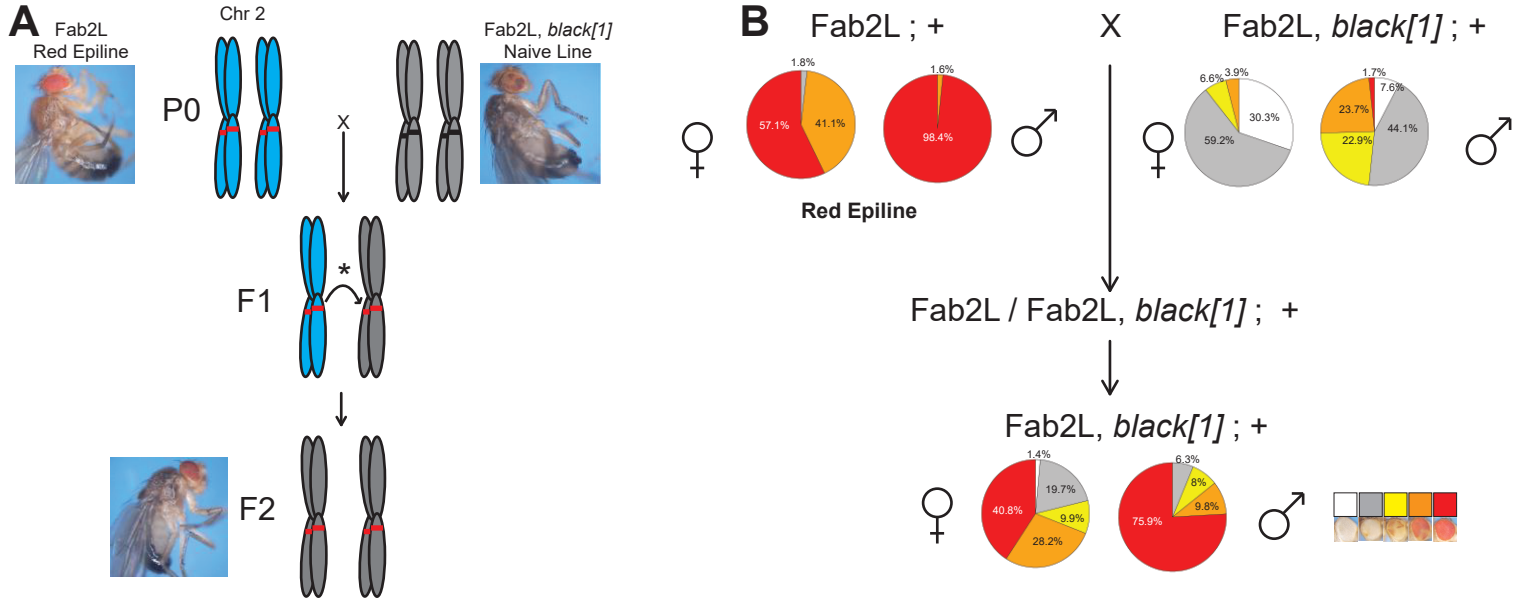


Figure S4

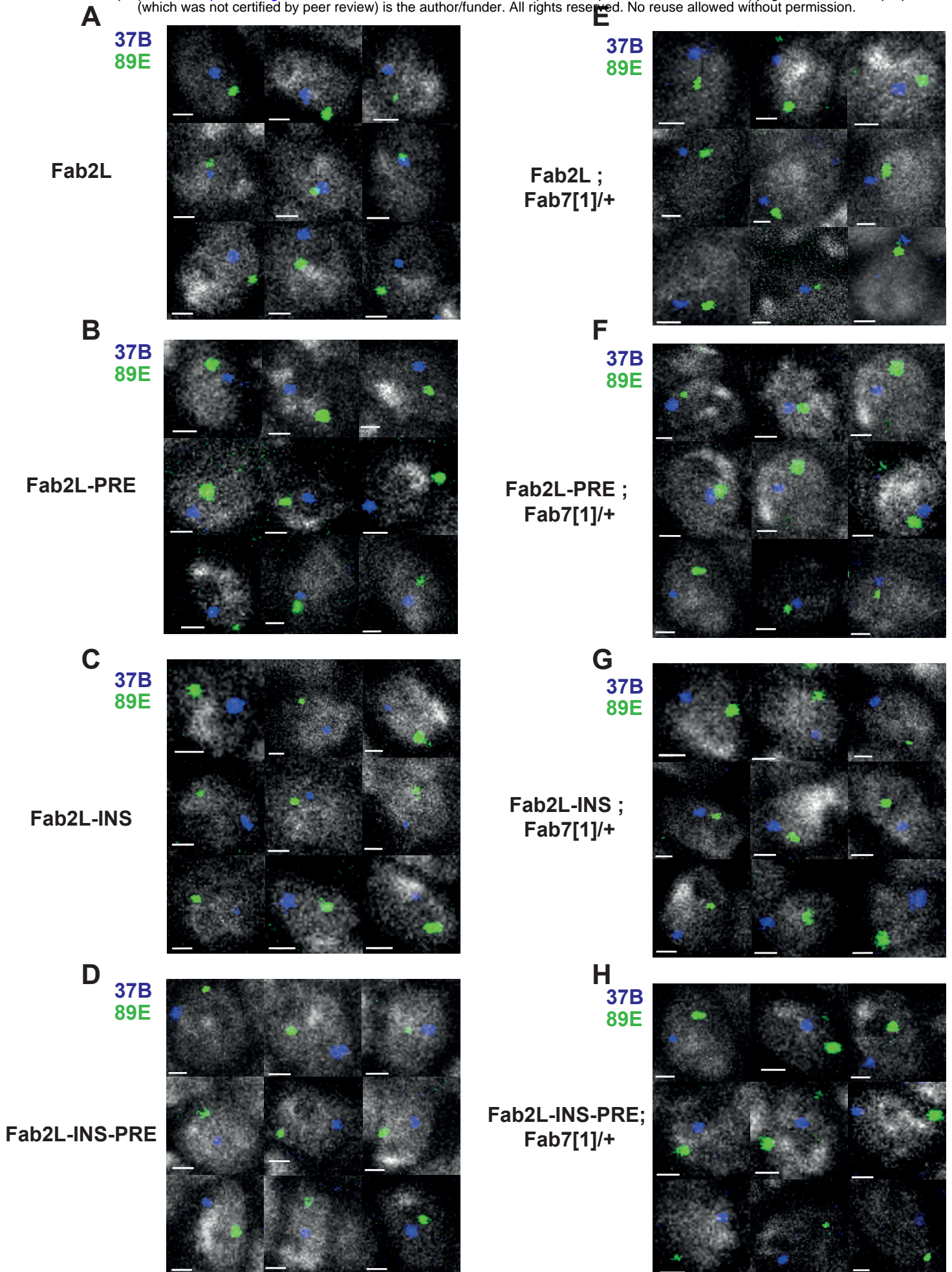


Figure S5

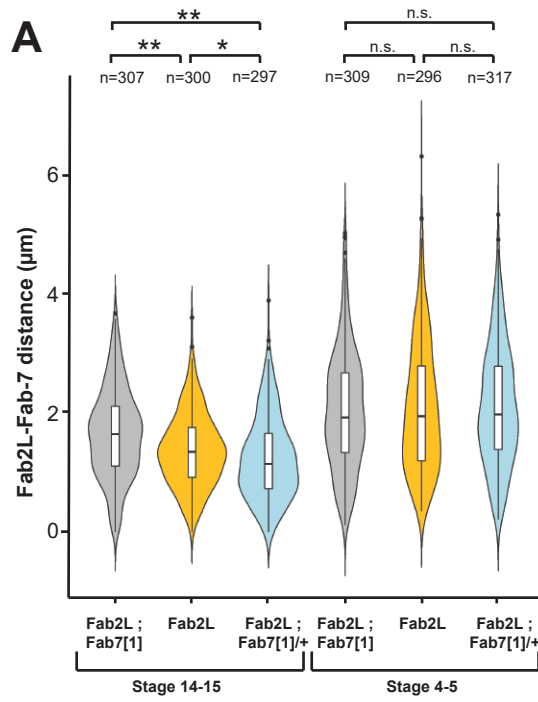


Figure S6

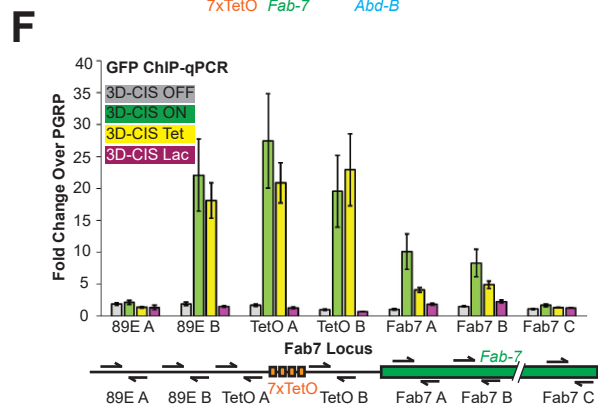
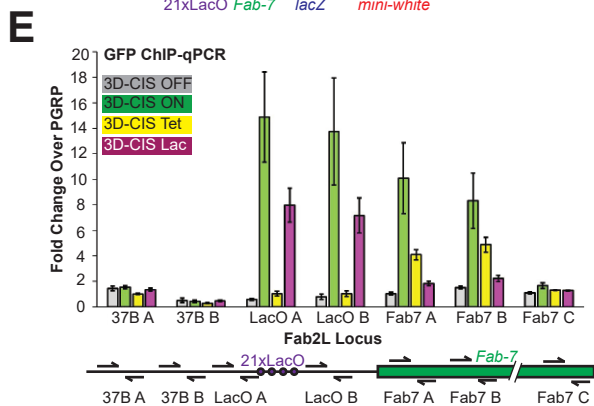
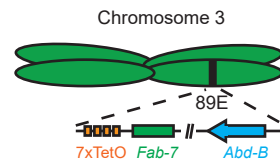
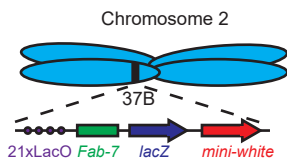
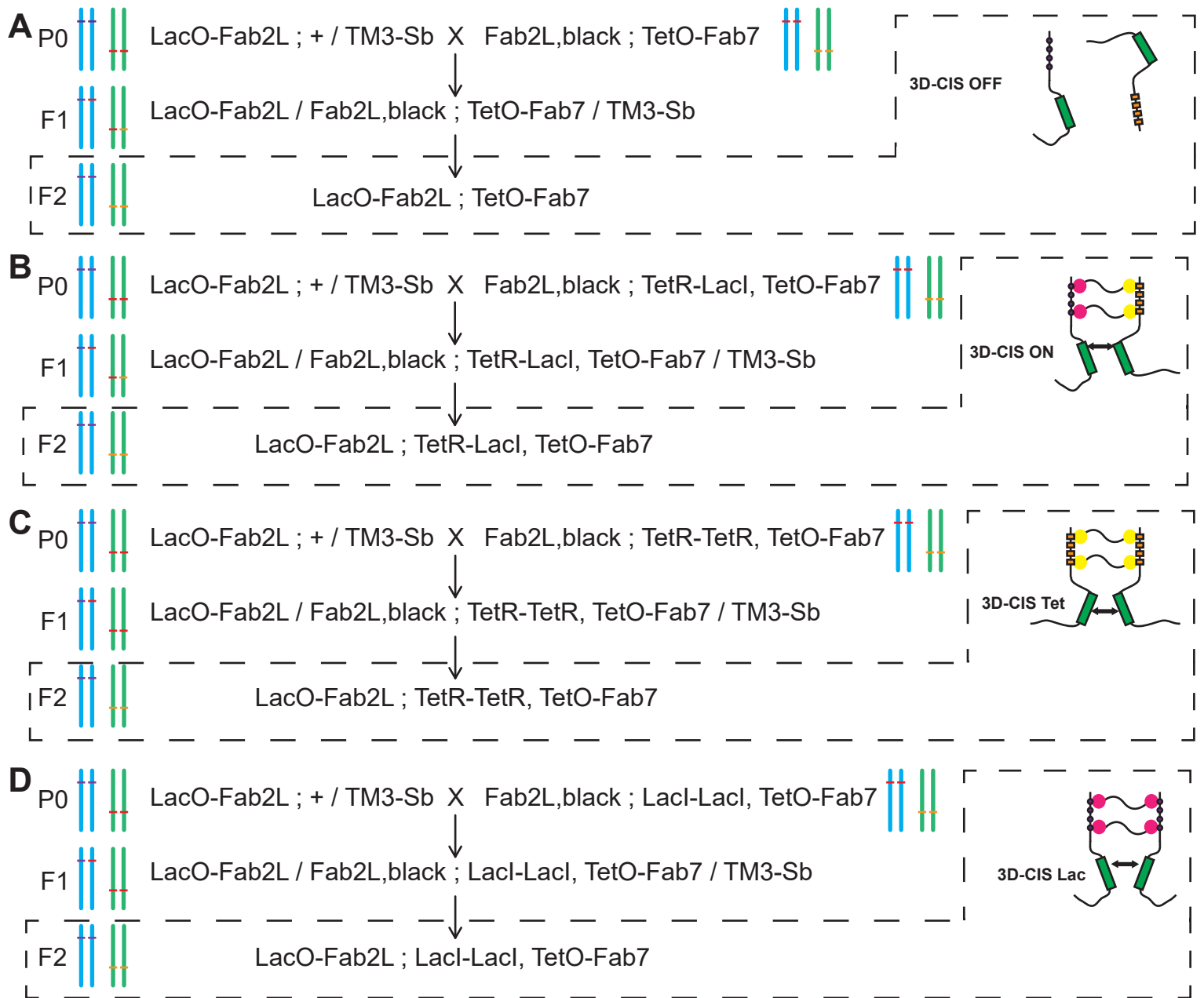


Figure S7

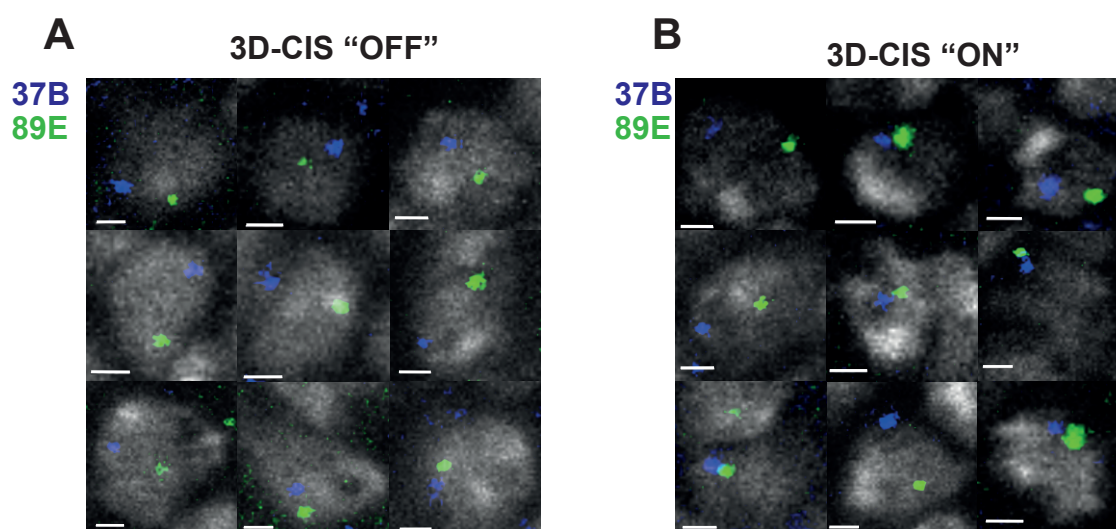


Figure S8

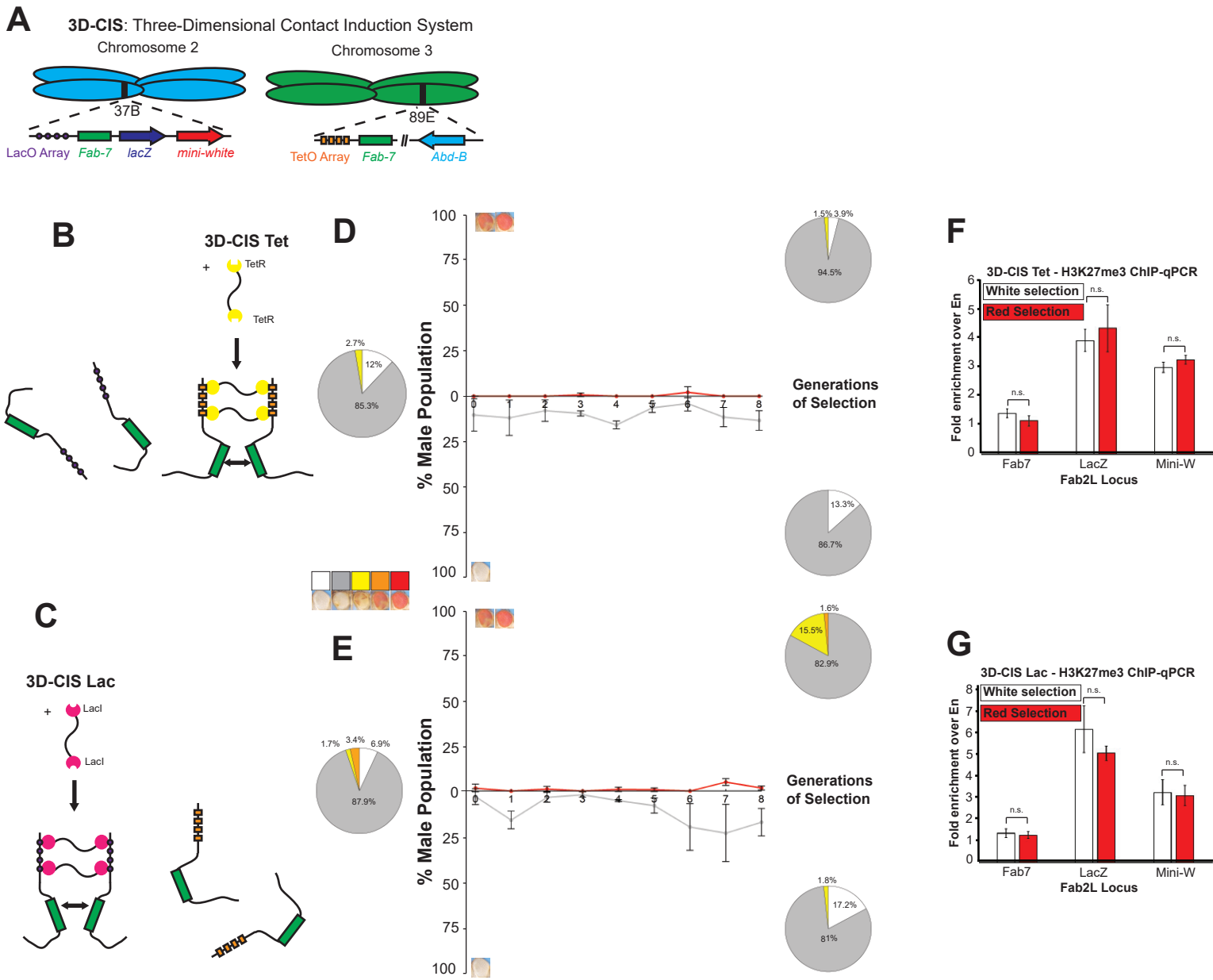
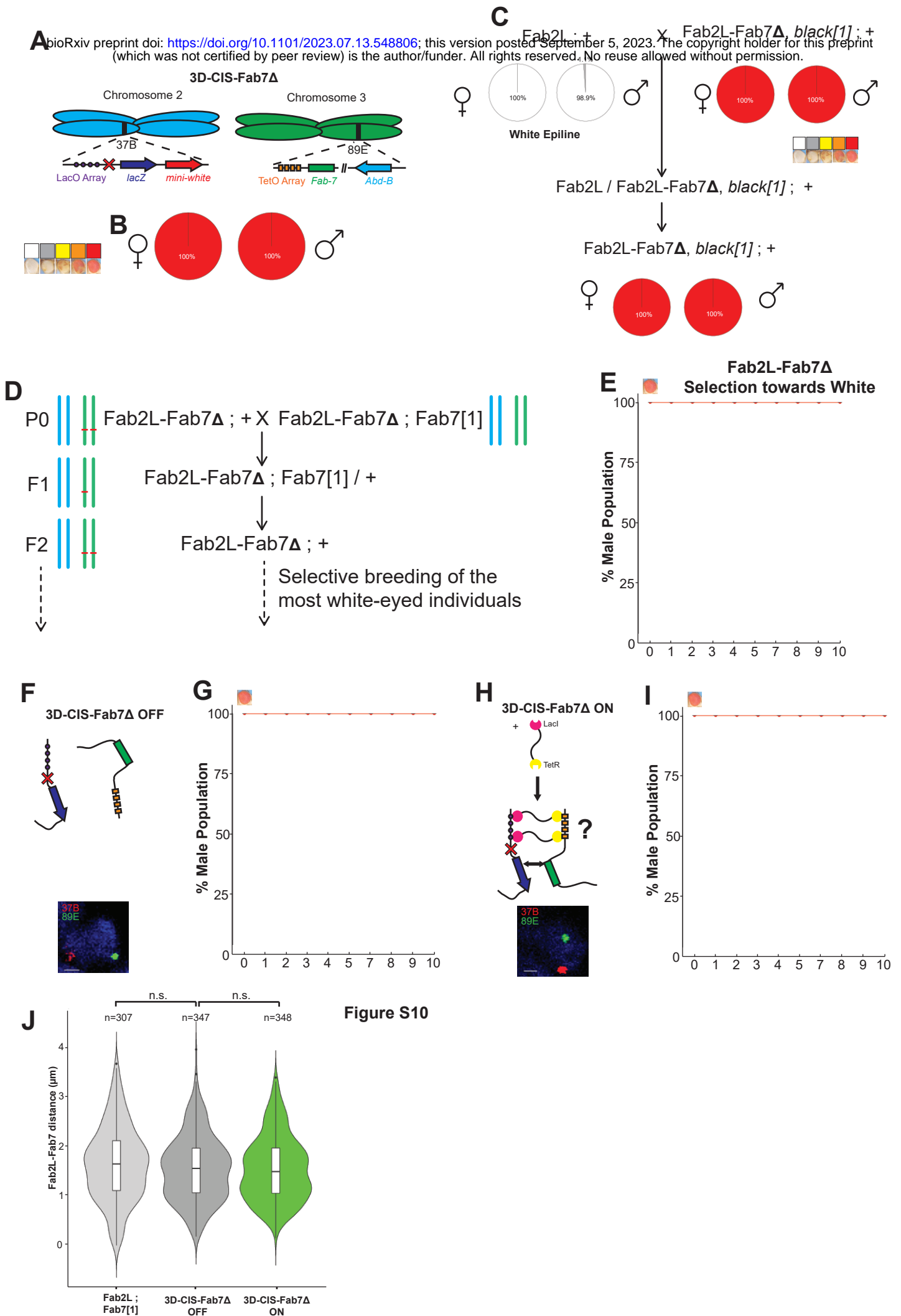


Figure S9



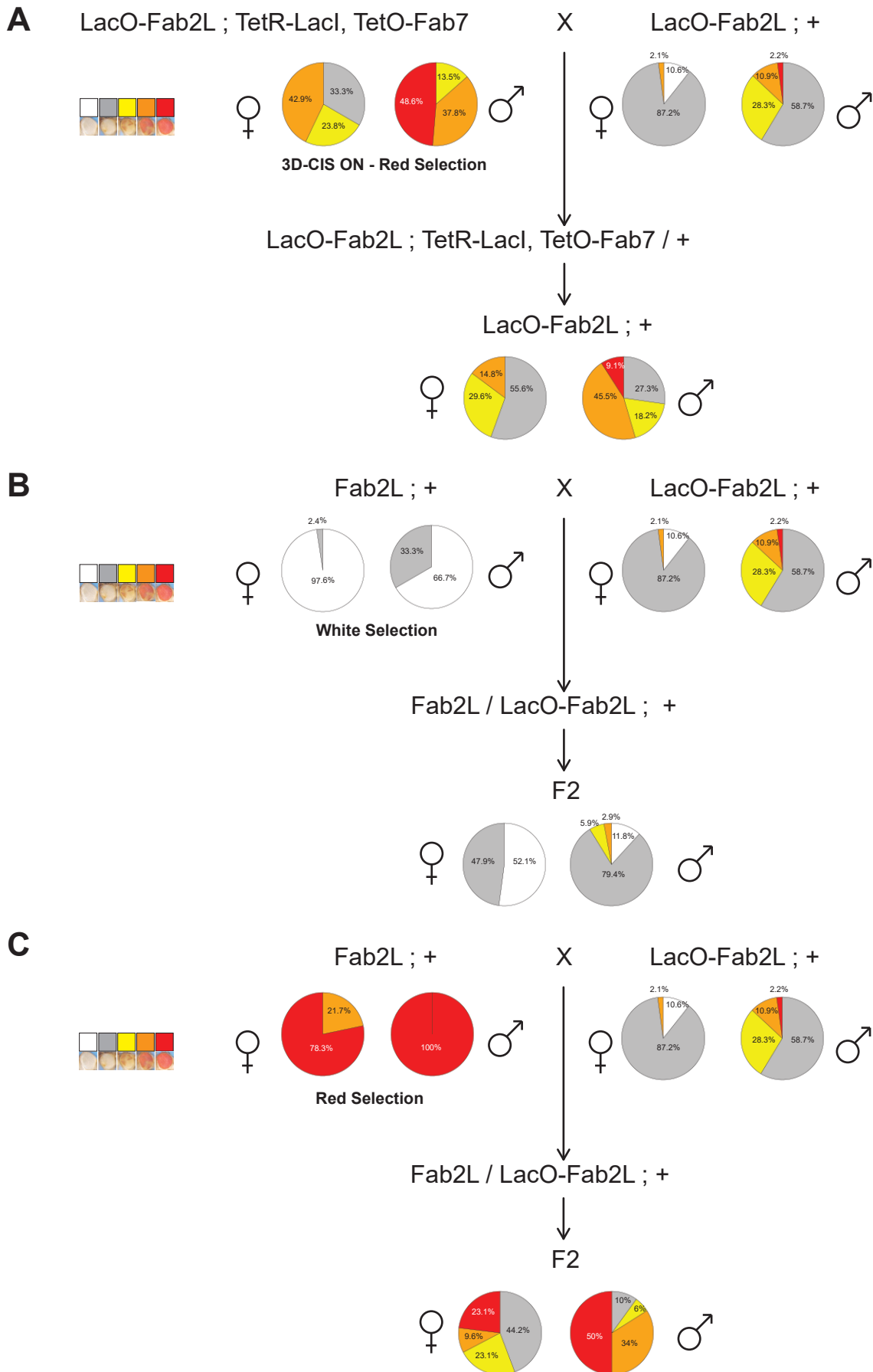


Figure S11